AD-A115 747 MISSION RESEARCH CORP SANTA BARBARA CA F/G 20/14
HF GROUND WAVE PROPAGATION OVER SMOOTH AND IRREGULAR TERRAIN.(U)
APR 81 G J FULKS DNA001-80-C-0022
UNCLASSIFIED MRC-R-621 DNA-5796F NL

1 of 1
AD A
115747

END
DATE
FILMED
7 82
DTIC

(12)

DNA 5796F

HF GROUND WAVE PROPAGATION OVER SMOOTH AND IRREGULAR TERRAIN

Gordon J. Fulks

Mission Research Corporation
P.O. Drawer 719
Santa Barbara, California 93102

30 April 1981

AD A115747

Final Report for Period 1 January 1980—30 April 1981

CONTRACT No. DNA 001-80-C-0022

APPROVED FOR PUBLIC RELEASE;
DISTRIBUTION UNLIMITED.

THIS WORK SPONSORED BY THE DEFENSE NUCLEAR AGENCY
UNDER RDT&E RMSS CODE X322080469 Q94QAXHB05301 H2590D.

Prepared for
Director
DEFENSE NUCLEAR AGENCY
Washington, D. C. 20305

UNCLASSIFIED

SECURITY CLASSIFICATION OF THIS PAGE (When Data Entered)

REPORT DOCUMENTATION PAGE		READ INSTRUCTIONS BEFORE COMPLETING FORM
1. REPORT NUMBER DNA 5796F	2. GOVT ACCESSION NO.	3. RECIPIENT'S CATALOG NUMBER
4. TITLE (and Subtitle) HF GROUND WAVE PROPAGATION OVER SMOOTH AND IRREGULAR TERRAIN		5. TYPE OF REPORT & PERIOD COVERED Final Report for Period 1 Jan 80 - 30 Apr 81
		6. PERFORMING ORG. REPORT NUMBER MRC-R-621
7. AUTHOR(s) Gordon J. Fulks		8. CONTRACT OR GRANT NUMBER(s) DNA 001-80-C-0022
9. PERFORMING ORGANIZATION NAME AND ADDRESS Mission Research Corporation P.O. Drawer 719 Santa Barbara, California 93102		10. PROGRAM ELEMENT, PROJECT, TASK AREA & WORK UNIT NUMBERS Subtask Q94QAXHB053-01
11. CONTROLLING OFFICE NAME AND ADDRESS Director Defense Nuclear Agency Washington, D.C. 20305		12. REPORT DATE 30 April 1981
		13. NUMBER OF PAGES 66
14. MONITORING AGENCY NAME & ADDRESS(if different from Controlling Office)		15. SECURITY CLASS. (of this report) UNCLASSIFIED
		15a. DECLASSIFICATION/DOWNGRADING SCHEDULE N/A

16. DISTRIBUTION STATEMENT (of this Report)

Approved for public release; distribution unlimited.

17. DISTRIBUTION STATEMENT (of the abstract entered in Block 20, if different from Report)

18. SUPPLEMENTARY NOTES

This work sponsored by the Defense Nuclear Agency under RDT&E RMSS Code X322080469 Q94QAXHB05301 H2590D.

19. KEY WORDS (Continue on reverse side if necessary and identify by block number)

Ground Wave
HF
Propagation
Terrain
Refraction

20. ABSTRACT (Continue on reverse side if necessary and identify by block number)

This report addresses several aspects of ground wave propagation. Included are discussions of the general characteristics of ground waves as well as specific formulas for predicting ground wave field strengths at arbitrary locations from a standard transmitter. These formulas, from the work of Bremmer, apply to either vertical or horizontal polarization, to a smooth spherical earth, and to a wide variety of soil types. A computer program to evaluate the formulas is presented and sample results are given. Although this report concentrates on HF frequencies

20. ABSTRACT (Continued)

many of the results are applicable to a much wider range of frequencies.

Atmospheric refraction, which may enhance ground wave propagation, is discussed. Formulas for predicting refraction effects based on atmospheric temperature and humidity as well as temperature and humidity gradients are presented.

Propagation over inhomogeneous and irregular terrain is considered. Only limited aspects of such propagation are discussed with an emphasis on irregular terrain. Obstacle gain is covered in some detail.

Because of the lack of experimental data for ground wave propagation over irregular terrain at HF frequencies, an experiment is recommended.

TABLE OF CONTENTS

LIST OF ILLUSTRATIONS

LIST OF ILLUSTRATIONS (continued) | Page

Figure

SECTION 1
INTRODUCTION

Ground wave propagation is possible at all radio frequencies but often neglected in the HF band (3-30 MHz) because of the much longer paths possible with sky wave propagation. Typical ground wave propagation paths are measured in tens to hundreds of kilometers while typical sky wave paths extend to thousands of kilometers. The purpose of this paper is to consider various aspects of HF ground wave propagation over smooth and irregular terrain. Although HF frequencies are emphasized, many of the results are applicable to a much wider range of frequencies.

A military situation involving a large nuclear exchange is one example where ground waves may be considerably more effective than sky waves. Nuclear explosions cause severe D-region absorption which can reduce or eliminate conventional HF sky wave modes. These explosions are expected to have little or no effect upon ground waves. While sky waves can be degraded by attacking the propagation medium (the ionosphere) such a tactic is nearly impossible with ground waves. Ground waves propagate along the ground/air interface and are only sensitive to substantial changes in this interface. Even a large nuclear exchange would not be expected to greatly alter the basic topography of a region and hence, the ground wave propagation.

On the other hand, ground wave propagation is vulnerable to jamming or to direct destruction of the terminals as is sky wave propagation. However, jamming of ground wave circuits can be made difficult by taking advantage of the limited range of ground waves. If sky wave propagation is suppressed by proper choice of frequencies and antennas, then an enemy must place a jammer near or within sight of the terminals being used to effectively jam them.

Ground wave propagation generally requires as much or more transmitter power and as good or better antennas than sky wave propagation. Higher transmitter power enhances enemy direction finding and eavesdropping but is compensated by the relatively small ground wave coverage regions. Because ground wave propagation is better at lower frequencies, it is tempting to consider operation at the low end of the HF band or even into the MF. However, efficient antennas at these frequencies are large and probably impractical for certain mobile applications. For these applications, it may be better to operate at middle HF frequencies where efficient antennas of moderate size are possible.

In general, ground wave propagation offers worthwhile capabilities for short distance military communications systems intended to survive a nuclear attack. Network communications systems with many closely spaced nodes may find ground waves attractive.

Because the subject of ground wave propagation is broad and complex, this report concentrates on those aspects which have recently been studied for DNA. An extensive survey of the ground wave literature has been made leading to the selection of a theoretical formalism appropriate to computer coding. The formalism chosen was developed by Hendricus Bremmer over 30 years ago and applies to propagation over a smooth spherical earth. This formalism has been coded in Fortran IV and is reported here. The computer routine has been kept relatively simple and does not yet include corrections for atmospheric refraction or for rough earth cases. These subjects are, however, discussed in some detail. Finally, the lack of experimental data is discussed along with a suggestion for a future experiment.

This work was supported by two DNA contracts: DNA 001-80-C-0022 and DNA 001-80-C-0225.

SECTION 2
GENERAL CONSIDERATIONS

There is often confusion as to the physical reality of ground waves (or surface or terrestrial waves). They are that portion of electromagnetic waves propagated through space and affected by the presence of the ground. They do not include any portion of the wave reflected from anything other than the ground. For example, ionospheric sky waves or tropospheric waves are separate phenomena. Line-of-sight propagation between two spacecraft in empty space away from the earth is also a separate phenomenon although "line-of-sight" propagation between two aircraft aloft is technically ground wave propagation. As the aircraft fly higher, ground wave propagation approaches line-of-sight propagation. In other words, the dielectric properties (dielectric constant and conductivity) as well as the topology of the ground influence the propagation of electromagnetic waves "near" the ground. "Near" is defined in terms of the number of wavelengths that the transmitter and receiver are above the ground. At two meters above the ground, visible light is hardly affected at all by the ground while HF transmissions are strongly affected.

Ground wave propagation is a diffraction effect but not one of the simpler diffraction effects often considered in the study of optics.[2] Although the general concept of diffraction around an edge applies to ground wave propagation around the earth, the mathematical formalism is considerably more complex for ground wave propagation. At one time, this subject was considered to be among the most difficult in theoretical physics. To obtain any solution at all requires several assumptions.

Arnold Sommerfeld solved the general problem of radio propagation from a short vertical antenna over a finitely conducting plane earth in 1909.[3] The rigorous results obtained by Sommerfeld were applicable to short transmission distances where the curvature of the earth could be ignored. It was already known that the solution for a spherical earth could be obtained in terms of a series of zonal harmonics. Unfortunately, this series converged so poorly that no practical results could be obtained for radio waves.

In 1918, Watson[4] developed a transformation with the aid of an integral in the complex plane which transformed the solution in terms of zonal harmonics into a residue series which converged rapidly and could be evaluated numerically. From 1926 through 1931, Sommerfeld, Van der Pol, Niessen, and Wise obtained several independent solutions of the problem using Watson's transformation. During this period, a fundamental error was also uncovered and corrected in Sommerfeld's original work. In the mid-1930's, Bremmer and Van der Pol in Europe and Norton in the United States extended the early work to the point where it became practical to use.[5,6,7,8,9,10] They simplified the mathematics, performed extensive numerical computations, and helped to better define the physical nature of ground waves. After the Second World War, many other investigators considered various aspects of the problem such as an inhomogeneous or rough earth. The most generally useful results, however, are still those of Bremmer or Norton. We have arbitrarily chosen to follow Bremmer's formalism[1] because it appears to be the easiest to use.

Bremmer's calculations reveal several general characteristics of ground waves. For instance, they propagate much better over water than over land, and better over wet land than dry land because the high conductivity of water and wet land produces less absorption. Ground waves are more influenced by the conductivity of the ground (soil type) than by the curvature of the earth (for transmitter and receiver on the earth). They are not abruptly changed by the horizon. As with most diffraction processes, there are no distinct shadows behind obstacles such as the horizon. Also, long wavelengths propagate farther around the earth than do short wavelengths. Ground waves are usually vertically polarized because horizontal polarization is readily short-circuited by the earth. Hence, horizontally polarized antennas such as might be used for sky wave propagation are relatively ineffective for ground wave propagation.

SECTION 3
BREMMER'S EQUATIONS/GROUND WAVE PROGRAM

This section presents a summary of Bremmer's approach to ground wave theory and shows how this theory has been used to create a simple computer routine for computing ground wave field intensities around a smooth spherical earth.

As mentioned in the last section, the rigorous theory for wave propagation around a sphere is a special application of diffraction theory. It is mathematically difficult because of the finite size of the sphere. Much simpler solutions are possible for a very small or large sphere. The general solution in terms of a series of zonal harmonics is given by[11]

$$H = \frac{IL}{cb}\left[\frac{e^{ik_0 s}}{s} + ik_0 \sum_{n=0}^{\infty} (2n+1) R_n \frac{\psi_n(k_0 a)}{\zeta_n^{(1)}(k_0 a)} \zeta_n^{(1)}(k_0 b)\, \zeta_n^{(1)}(k_0 r)\, P_n(\cos\theta)\right] \quad (1)$$

where H is the magnitude of Hertzian vector. This Hertzian vector is related to the conventional vector potential, $\vec{A}$, by the relation

$$\vec{\Pi} = H\hat{r} = \frac{1}{\mu}\vec{A} = \frac{i}{\omega\mu}\frac{\partial\vec{A}}{\partial t} \quad (2)$$

From a knowledge of the Hertzian vector, the electric and magnetic field components follow directly.

The effective reflection coefficient in (1) is defined by

$$R_n = \frac{-\frac{1}{x}\frac{d}{dx}\ \ln\ [x\Psi_n(x)]_{\ x=k_0a} + \frac{1}{x}\frac{d}{dx}\ \ln\ [x\Psi_n(x)]_{\ x=k_1a}}{\frac{1}{x}\frac{d}{dx}\ \ln\ [x\zeta_n^{(1)}(x)]_{\ x=k_0a} - \frac{1}{x}\frac{d}{dx}\ \ln\ [x\Psi_n(x)]_{\ x=k_1a}} \tag{3}$$

and the functions $\zeta_n{}^{(1)}(x)$ and $\Psi_n(x)$ are given by

$$\zeta_n{}^{(1)}(x) = \sqrt{\frac{\pi}{2x}}\quad H^{(1)}_{n+1/2}(x) = x^n\ \left(-\frac{1}{x}\frac{d}{dx}\right)^n\ \left(\frac{e^{ix}}{ix}\right) \tag{4}$$

$$\Psi_n(x) = \sqrt{\frac{\pi}{2x}}\ J_{n+1/2}(x) = x^n\ \left(-\frac{1}{x}\frac{d}{dx}\right)^n\ \left(\frac{\sin x}{x}\right) \tag{5}$$

where H and J are the conventional Hankel and Bessel functions. Other quantities in (1) are defined as

IL = *electric dipole moment of the* assumed small vertical dipole antenna

s = distance between transmitter and receiver

b = radial distance of antenna from center of assumed spherical coordinate system

k_0 ,k_1 = radial wave numbers outside and inside the earth

a = radius of sphere (in this case, the earth).

The numerical evaluation of (1) is very difficult and for a long time remained unknown. The problem is the convergence of the series for a finite radius, a. If a is small compared to the wavelength, the series converges rapidly, and the first term yields Rayleigh scattering. The greater the value of the parameter $k_1a = 2\pi a/\lambda$, the more slowly the series converges. The most significant terms are those of order $n \approx k_1a$. In the radio case, k_1a varies from 10^3 to 10^9 requiring the summation of a great number of terms.

Because such a summation is impractical, Watson developed a transformation which converted (1) into a contour integral in the complex n-plane. This reduced the problem to a summation of residues which can be mastered numerically. Bremmer introduced approximations for the resulting Hankel functions and zonal harmonics leading to a simpler expression for the r.m.s. value of the electric field at a distance, D_{km}, from a short vertical dipole antenna.[1] That expression is shown below with two significant modifications to bring these computations in line with the conventions of the CCIR (see Appendix). The electric field has been normalized to give a value of 346.4 mv/m at 1 km if the assumed dipole transmitting antenna is placed on a perfectly conducting plane earth. The same dipole antenna will give a field of 173.2 mv/m at 1 km in free space which is the free space field from a 1 kw isotropic antenna. Bremmer and others use 300 mv/m instead of 346.4 which corresponds to the field from a dipole antenna radiating 1 kw over a perfectly conducting plane earth. The antenna assumed here radiates 4/3 kw under these conditions. Another modification to Bremmer's equations involves the distance D_{km}. While Bremmer uses straight line and great circle distance equivalently, the following expressions use the latter only.

$$E = \left[346.4\sqrt{2\pi\chi}\,/\sqrt{(h_1+a)^2 + (h_2+a)^2 - 2(h_1+a)\,(h_2+a)\cos\,(D_{km}/a)}\right]$$

$$\times \left| \sum_{s=0}^{\infty} f_s(h_1)\, f_s(h_2)\, e^{i\tau_s\chi}/(2\tau_s - 1/\delta^2) \right| \qquad \text{mv/m} \qquad (6)$$

where

D_{km} = distance along the surface of the earth from transmitter to receiver in km.

χ = $.053693\, D_{km}/\lambda_m{}^{1/3}$ (7)

λ_m = wavelength in m

$f_s(h_1)$ = height gain factor

$$= \left(\frac{x_1^2 - 2\tau_s}{-2\tau_s}\right)^{1/2} \frac{H_{1/3}^{(1)}\ [\frac{1}{3}\ (x_1{}^2 - 2\tau_s)^{3/2}]}{H_{1/3}^{(1)}\ [\frac{1}{3}\ (-2\tau_s)^{3/2}]} \tag{8}$$

$x_1{}^2 = .03674\ h_1/\lambda_m^{2/3}$

h_1 = height of transmitter above ground in m

h_2 = height of receiver in m

$$\delta_e = K_e^{\ i(135° - \psi_e)} \tag{9}$$

$$K_e = .002924\ \lambda_m{}^{1/3} \frac{\sqrt{\varepsilon^2 + 3.6 \times 10^{25} \sigma_e^2\ \lambda_m^2}}{\sqrt[4]{(\varepsilon - 1)^2 + 3.6 \times 10^{25} \sigma_e^2\ \lambda_m^2}} \tag{10}$$

$$\psi_e = \tan^{-1}\left(\frac{\varepsilon}{6 \times 10^{12}\ \sigma_e \lambda_m}\right) - \frac{1}{2} \tan^{-1}\left(\frac{\varepsilon - 1}{6 \times 10^{12}\ \sigma_e\ \lambda_m}\right) \tag{11}$$

The values of τ_s follow from

$$\tau_s = \text{Re}\ \tau_s + i\ \text{Im}\ \tau_s \tag{12}$$

and assuming K_e is small:

$$\text{Re}\ \tau_0 = .928 + K_e \cos(45° + \psi_e) + 1.237\ K_e{}^3 \cos(75° + 3\psi_e) - .5\ K_e{}^4 \cos(4\psi_e) - 2.755\ K_e{}^5 \cos(75° - 5\psi_e) \ldots$$

$$\text{Re}\ \tau_1 = 1.622 + K_e \cos(45° + \psi_e) + 2.163\ K_e{}^3 \cos(75° + 3\psi_e) - .5\ K_e{}^4 \cos(4\psi_e) - 8.422\ K_e{}^5 \cos(75° - 5\psi_e) \ldots$$

$$\mathrm{Re}\ \tau_2 = 2.191 + K_e \cos(45° + \Psi_e) + 2.921\ K_e^{\,3} \cos(75° + 3\Psi_e) - .5\ K_e^{\,4} \cos(4\Psi_e) - 15.36\ K_e^{\,5} \cos(75° - 5\Psi_e) \ldots$$

$$\mathrm{Re}\ \tau_3 = 2.694 + K_e \cos(45° + \Psi_e) + 3.592\ K_e^{\,3} \cos(75° + 3\Psi_e) - .5\ K_e^{\,4} \cos(4\Psi_e) - 23.227\ K_e^{\,5} \cos(75° - 5\Psi_e) \ldots$$

$$\begin{aligned}\mathrm{Re}\ \tau_s = {} & 1.116\ (s + 3/4)^{2/3} + K_e \cos(45° + \Psi_e) \\ & + 1.488\ (s + 3/4)^{2/3} K_e^{\,3} \cos(75° + 3\Psi_e) \\ & - .5\ K_e^{\,4} \cos(4\Psi_e) \\ & - 3.987\ (s + 3/4)^{4/3} K_e^{\,5} \cos(75° - 5\Psi_e) \ldots \qquad \text{for } s > 3\end{aligned}$$

$$\mathrm{Im}\ \tau_0 = 1.607 - K_e \sin(45° + \Psi_e) - 1.237\ K_e^{\,3} \sin(75° + 3\Psi_e) + .5\ K_e^{\,4} \cos(4\Psi_e) - 2.755\ K_e^{\,5} \cos(75° - 5\Psi_e) \ldots$$

$$\mathrm{Im}\ \tau_1 = 2.810 - K_e \sin(45° + \Psi_e) - 2.163\ K_e^{\,3} \sin(75° + 3\Psi_e) + .5\ K_e^{\,4} \sin(4\Psi_e) - 8.422\ K_e^{\,5} \sin(75° - 5\Psi_e) \ldots$$

$$\mathrm{Im}\ \tau_2 = 3.795 - K_e \sin(45° + \Psi_e) - 2.921\ K_e^{\,3} \cos(75° + 3\Psi_e) + .5\ K_e^{\,4} \sin(4\Psi_e) - 15.36\ K_e^{\,5} \sin(75° - 5\Psi_e) \ldots$$

$$\mathrm{Im}\ \tau_3 = 4.663 + K_e \sin(45° + \Psi_e) + 3.592\ K_e^{\,3} \cos(75° + 3\Psi_e) + .5\ K_e^{\,4} \sin(4\Psi_e) - 23.227\ K_e^{\,5} \sin(75° - 5\Psi_e) \ldots$$

$$\text{Im}\ \tau_s = 1.932(s + 3/4)^{2/3} - K_e \sin(45° + \Psi_e)$$
$$- 1.488(s + 3/4)^{2/3} K_e^3 \sin(75° + 3\Psi_e)$$
$$+ .5\ K_e^4 \sin(4\Psi_e)$$
$$- 3.987(s + 3/4)^{4/3} K_e^5 \sin(75° - 5\Psi_e) \ldots \qquad \text{for } s > 3$$

For K_e large:

$$\text{Re}\ \tau_0 = .4043 + .6183 \frac{\cos(15° - \Psi_e)}{K_e} - .2364 \frac{\sin(2\Psi_e)}{K_e^2}$$
$$- .0533 \frac{\cos(15° + 3\Psi_e)}{K_e^3} + .00226 \frac{\cos(60° - 4\Psi_e)}{K_e^4} \ldots$$

$$\text{Re}\ \tau_1 = 1.288 + .194 \frac{\cos(15° - \Psi_e)}{K_e} - .0073 \frac{\sin(2\Psi_e)}{K_e^2}$$
$$+ .0120 \frac{\cos(15° - 3\Psi_e)}{K_e^3} - .00160 \frac{\cos(60° - 4\Psi_e)}{K_e^4} \ldots$$

$$\text{Re}\ \tau_s \approx 1.116\ (s + 1/4)^{2/3} + \frac{.2241}{(s + 1/4)^{2/3}} \frac{\cos(15° - \Psi_e)}{K_e} \ldots$$
$$\text{for } s > 1$$

$$\text{Im}\ \tau_0 = .7003 - .6183 \frac{\sin(15° - \Psi_e)}{K_e} + .2364 \frac{\cos 2\Psi_e}{K_e^2}$$
$$- .0533 \frac{\sin(15° + 3\Psi_e)}{K_e^3} - .00226 \frac{\sin(60° - 4\Psi_e)}{K_e^4} \ldots$$

$$\text{Im}\,\tau_1 = 2.232 - .1940\,\frac{\sin(15^\circ - \Psi_e)}{K_e} + .0073\,\frac{\cos(2\Psi_e)}{K_e{}^2}$$

$$+ .0120\,\frac{\sin(15^\circ + 3\Psi_e)}{K_e{}^3} + .00160\,\frac{\sin(60^\circ - 4\Psi_e)}{K_e{}^4} \ldots$$

$$\text{Im}\,\tau_s \approx 1.932\,(s + 1/4)^{2/3} - \frac{.2241}{(s + 1/4)^{2/3}}\,\frac{\sin(15^\circ - \Psi_e)}{K_e} \ldots \quad \text{for } s>1$$

These expressions apply to a vertical dipole transmitting antenna and to a separation between transmitter and receiver of at least

$$D_{km} > 5\,\lambda_m{}^{1/3}.$$

For a horizontal dipole antenna, the above equations can be used (in the direction of the maximum field) providing that δ_e, K_e, and ψ_e are replaced by δ_m, K_m, and $90^\circ - \Psi_m$. These latter quantities are defined as follows:

$$\delta_m = K_m\, e^{i(45^\circ + \Psi_m)} \tag{13}$$

$$K_m = .002924\,\frac{\lambda_m{}^{1/3}}{\sqrt[4]{(\varepsilon - 1)^2 + 3.6 \times 10^{25}\,\sigma_e{}^2\,\lambda_m{}^2}} \tag{14}$$

$$\Psi_m = \frac{1}{2}\,\tan^{-1}\left(\frac{\varepsilon - 1}{6 \times 10^{12}\,\sigma_e\,\lambda_m}\right) \tag{15}$$

It should also be noted that σ_e is defined in terms of e.m.u. following Bremmer's preference. In terms of more customary usage, this can be written as

$$\underset{\text{e.m.u.}}{\sigma_e} = 10^{11}\,\underset{\text{mhos/m}}{\sigma_\Omega} \; .$$

The height gain factors in (6) and (8) are made up of Hankel functions. Using Bremmer's approximation for these functions, they can be written as

a) for $h_{1m} > 50\ \lambda_m^{2/3}$ (approximately):

$$f_s(h_1) = \frac{A_s}{\delta_e \sqrt[4]{x_1^{\,2} - 2\tau_s}} \left\{ e^{\left[-\,i\pi/4 + \frac{i}{3}\,(x_1^{\,2} - 2\tau_s)^{3/2}\right]} \times \right. \tag{16}$$

$$\left[1 - i\,\frac{.2038}{(x_1^{\,2} - 2\tau_s)^{3/2}} - \frac{.3342}{(x_1^{\,2} - 2\tau_s)^{3}} \cdots \right] -$$

$$\left. e^{\left[i\pi/4 - \frac{i}{3}\,(x_1^{\,2} - 2\tau_s)^{3/2}\right]} \left[1 + i\,\frac{.2083}{(x_1^{\,2} - 2\tau_s)^{3/2}} \cdots \right] \right\}$$

where

$$\begin{aligned} A_0 &= .3582\ e^{i\ 120^\circ} \\ A_1 &= .3129\ e^{-i\ 60^\circ} \\ A_2 &= .2903\ e^{i\ 120^\circ} \\ A_3 &= .2760\ e^{-i\ 60^\circ} \\ A_s &= .3440\ \frac{(-1)^{s+1}}{(s + 3/4)^{1/6}}\ e^{-i\pi/3} \qquad \text{for } s > 3 \end{aligned} \tag{17}$$

b) for $h_{1m} < 50\ \lambda_m^{2/3}$ (approximately):

$$f_s(h_1) = 1 + 6.283\ \left(\frac{1}{x^{1/3}\ \delta_e} - \frac{1}{x}\right) \frac{h_1}{\lambda} - 39.48\ \frac{(1 - x^{2/3}\ \delta_e\ \tau_s)}{x^{4/3}\ \delta_e} \left(\frac{h_1}{\lambda}\right)^2 \cdots \tag{18}$$

where

$$x = \frac{4\times10^7}{\lambda_m}$$

The height gain factor for the receiver $f_s(h_2)$ can be computed as above by substituting h_2 for h_1. Similarly, the height gain factors for a horizontal dipole can be computed from the equations above by substituting δ_m for δ_e. Bremmer maintains that methods (a) and (b) above are sometimes equally suitable.

Using equations (6) through (18), a ground wave program has been constructed and is given in Table 1. By modifying the input and output, this program has also been converted into a subroutine for the nuclear effects code known as HFNET. The necessary inputs (including units) are shown in the program listing. This program applies to ground wave propagation around a smooth homogeneous spherical earth. It does not contain any provisions for a rough or inhomogeneous earth. It also does not contain the effects of atmospheric refraction. Despite these limitations, the program accurately computes ground wave field strengths in many practical cases where there are no large departures from the assumptions built into the program. The program is not limited to the HF band but applies to a wide range of radio frequencies. It has been checked out from 15 KHz to 100 GHz but may be applicable to an even wider range of frequencies. It is also applicable to a wide range of separations between transmitter and receiver. As will be shown below, the routine does fail under some circumstances where the transmitter and receiver are close together (in terms of number of wavelengths) or high above the earth in full view of each other. Under these conditions, a "geometric optical" model is more appropriate and will be added to the program in the future. Although the residue series model used in this program is relatively less efficient when the receiver is in view of the transmitter, the results are still accurate except as noted. Many more terms in the residue series need to be summed when the receiver is above the transmitter's geometrical horizon.

Extensive checkout of the ground wave program has been accomplished and is shown in Figures 1 through 8. (All of this checkout was

Table 1. Ground wave program listing.

```
C           PROGRAM: GROUND WAVE
C
C           ****************************************
C
C           BREMMER GROUND WAVE MODEL
C
C           CODED BY GORDON J. FULKS     4/80
C
C           ****************************************
            DIMENSION TAUR(0:3), TAUI(0:3), HT(2), CSQ(2)
            REAL K,K2,K3,K4,K5,LAMBDA
            COMPLEX  DELTA, J,  A(0:3), DIF, F1, F2, AX
            COMPLEX SUM, F3, SUMX, SSDIF, HGF(2), TAU
            OPEN (UNIT=1,NAME='GND.DAT',TYPE='OLD',READONLY)
            OPEN (UNIT=2,NAME='GND.OUT',TYPE='NEW')
            C1 = 1./3.
            C2 = 2. * C1
            C3 = 4. * C1
            C4 = C1 / 2.
            J = CMPLX(0.,1.)
            PI = 3.1415926535
            RAD = 6.371E3
C           ****************************************
C
C           INPUT SECTION
C
C           ****************************************
C
C           READ TRANSMITTER POWER IN KILOWATTS, TRANSMITTER WAVELENGTH
C           IN METERS, AND GREAT CIRCLE DISTANCE ALONG THE SURFACE OF
C           THE EARTH FROM TRANSMITTER TO RECEIVER IN KILOMETERS
C
            READ (1,*) PWR, LAMBDA, D
C
C           READ HEIGHTS OF TRANSMITTER AND RECEIVER ABOVE THE GROUND
C           IN METERS AND WHETHER THEY ARE VERTICALLY OR HORIZONTALLY
C           POLARIZED (0 - VERTICAL, 1 = HORIZONTAL)
C
            READ (1,*) HT, NPOL
C
C           READ GROUND CHARACTERISTICS
C              EPSLN = RELATIVE DIELECTRIC CONSTANT
C              SIGMA = CONDUCTIVITY IN MHOS/METER
C
            READ (1,*) EPSLN, SIGMA
C           ****************************************
C
C           COMPUTATION SECTION
C
C           ****************************************
            SIGMA = SIGMA * 1.E-11
            CHI = .053693 * D / LAMBDA**C1
            H1 = HT(1) * 1.E-3
            H2 = HT(2) * 1.E-3
            DIS = (H1 + RAD)**2 + (H2 + RAD)**2
            DIS = SQRT(DIS - 2*(H1 + RAD) * (H2 + RAD) * COS(D/RAD))
            K = .002924 * LAMBDA**C1
            K = K / SQRT(SQRT((EPSLN - 1.)**2 + 3.6E25 * SIGMA**2
            1 * LAMBDA**2))
            IF (NPOL.EQ.1) GO TO 50
            K = K * SQRT(EPSLN**2 + 3.6E25 * SIGMA**2 * LAMBDA**2)
            PSI = ATAN(EPSLN/(6.E12 * SIGMA * LAMBDA))
            PSI = PSI - .5 * ATAN((EPSLN - 1.) / (6.E12 * SIGMA * LAMBDA))
            DELTA = K * EXP(J * ((3. * PI / 4.) - PSI))
            GO TO 100
     50     PSI = .5 * ATAN((EPSLN - 1.) / (6.E12 * SIGMA * LAMBDA))
            DELTA = K * EXP(J * ((PI / 4.) + PSI))
            PSI = PI / 2. - PSI
C
C           RESIDUE SERIES
C
    100     K2 = K**2
```

Table 1. (Cont.)

```
              K3 = K**3
              K4 = K**4
              K5 = K**5
              IF (K.GT.0.6) GO TO 200
              ANG1 = (PI / 4.) + PSI
              ANG2 = 75. * PI / 180. + 3. * PSI
              ANG3 = 4. * PSI
              ANG4 = 75. * PI / 180. - 5. * PSI
              CANG1 = COS(ANG1)
              SANG1 = SIN(ANG1)
              CANG2 = COS(ANG2)
              SANG2 = SIN(ANG2)
              CANG3 = COS(ANG3)
              SANG3 = SIN(ANG3)
              CANG4 = COS(ANG4)
              SANG4 = SIN(ANG4)
              TAUR(0) = .928 + K*CANG1 + 1.237*K3*CANG2 - .5*K4*CANG3 -
              1 2.755*K5*CANG4
              TAUR(1) = 1.622 + K*CANG1 + 2.163*K3*CANG2 - .5*K4*CANG3 -
              1 8.422*K5*CANG4
              TAUR(2) = 2.191 + K*CANG1 + 2.921*K3*CANG2 - .5*K4*CANG3 -
              1 15.36*K5*CANG4
              TAUR(3) = 2.6937 + K*CANG1 + 3.5919*K3*CANG2 - .5*K4*CANG3 -
              1 23.2268*K5*CANG4
              TAUI(0) = 1.607 - K*SANG1 - 1.237*K3*SANG2 + .5*K4*SANG3 -
              1 2.755*K5*SANG4
              TAUI(1) = 2.810 - K*SANG1 - 2.163*K3*SANG2 + .5*K4*SANG3 -
              1 8.422*K5*SANG4
              TAUI(2) = 3.795 - K*SANG1 - 2.921*K3*SANG2 + .5*K4*SANG3 -
              1 15.36*K5*SANG4
              TAUI(3) = 4.6633 - K*SANG1 - 3.5919*K3*SANG2 + .5*K4*SANG3 -
              1 23.2268*K5*SANG4
              GO TO 300
       200    ANG1 = 15. * PI / 180. - PSI
              ANG2 = 2. * PSI
              ANG3 = 15. * PI /180 + 3. * PSI
              ANG4 = PI / 3. - 4. * PSI
              BCANG1 = COS(ANG1)
              BSANG1 = SIN(ANG1)
              CANG2 = COS(ANG2)
              SANG2 = SIN(ANG2)
              CANG3 = COS(ANG3)
              SANG3 = SIN(ANG3)
              CANG4 = COS(ANG4)
              SANG4 = SIN(ANG4)
              TAUR(0) = .4043 + .618*BCANG1/K - .2364*SANG2/K2 -
              1 .0533*CANG3/K3 + .00226*CANG4/K4
              TAUR(1) = 1.288 + .194*BCANG1/K - .0073*SANG2/K2 +
              1 .0120*CANG3/K3 - .00160*CANG4/K4
              TAUI(0) = .7003 - .6183*BSANG1/K + .2364*CANG2/K2 -
              1 .0533*SANG3/K3 - .00226*SANG4/K4
              TAUI(1) = 2.232 - .1940*BSANG1/K + .0073*CANG2/K2 +
              1 .0120*SANG3/K3 + .00160*SANG4/K4
              DO 230 I = 2,3
              TAUR(I) = 1.116*(I + .25)**C2 + .2241*BCANG1 /
              1 (K*(I + .25)**C2)
              TAUI(I) = 1.932*(I + .25)**C2 - .2241*BSANG1 /
              1 (K*(I + .25)**C2)
       230    CONTINUE
       C
       C      HEIGHT GAIN FACTORS
       C
       300    COM = 50. * LAMBDA**C2
              SUM = 0.
              E = 868.3 * SQRT(CHI) * 1.E3/DIS
              A(0) = .3582 * EXP(J * C2 * PI)
              A(1) = .3129 * EXP(-J * C1 *PI)
              A(2) = .2903 * EXP(J * C2 * PI)
              A(3) = .2760 * EXP(-J * C1 *PI)
              DO 399 N = 1,2
              CSQ(N) = .03674 * HI(N) / LAMBDA**C2
       399    CONTINUE
```

Table 1. (Cont.)

```
      DO 899 I = 0,500
      IF (I.GT.3) GO TO 410
      AX = A(I)
      TAU = CMPLX(TAUR(I),TAUI(I))
      GO TO 500
410   IF (K.GT.0.6) GO TO 450
      TAURX = 1.116*(I+.75)**C2 + K*CANG1 + 1.4881*(I+.75)**C2
     1 *K3*CANG2 - .5*K4*CANG3 - 3.9867*(I+.75)**C3*K5*CANG4
      TAUIX = 1.932*(I+.75)**C2 - K*SANG1 - 1.4881*(I+.75)**C2
     1 *K3*SANG2 + .5*K4*SANG3 - 3.9867*(I+.75)**C3*K5*SANG4
      GO TO 460
450   TAURX = 1.116*(I+.25)**C2 + .2241*BCANG1 /
     1 (K*(I+.25)**C2)
      TAUIX = 1.932*(I+.25)**C2 - .2241*BSANG1 /
     1 (K*(I+.25)**C2)
460   AX = .3440 * (-1)**(I+1) * EXP(-J * PI/3) / (I+.75)**C4
      TAU = CMPLX(TAURX, TAUIX)
500   DO 700 N=1,2
      IF (HT(N).LT.COM) GO TO 550
      DIF = CSQ(N) - 2. * TAU
      F1 = -J * PI/4. + J * ((SQRT(DIF))**3) / 3.
      F2 = 1. - J * 5./(24. * (SQRT(DIF))**3) - 385./(1152. * DIF**3)
      F3 = 1. + J * 5./(24. * (SQRT(DIF))**3)
      IF (ABS(REAL(F1)).GT.89.) GO TO 510
      HGF(N) = F2 * EXP(F1) - F3 * EXP(-F1)
      SSDIF = SQRT(SQRT(DIF))
      HGF(N) = HGF(N) * AX / (DELTA * SSDIF)
      GO TO 530
510   HGF(N) = 1.
530   CONTINUE
      GO TO 700
550   X = 4.E07 / LAMBDA
      HGF(N) = 1. + 6.283 * (1 / (DELTA * X**C1) - 1./X) *
     1 HT(N) / LAMBDA
      HGF(N) = HGF(N) - 39.48 * HT(N)**2 * (1. - X**C2 *
     1 DELTA * TAU) / (DELTA * LAMBDA**2 * X**C3)
700   CONTINUE
      SUMX =  HGF(1) * HGF(2) * EXP(J * TAU * CHI)
     1 / (2. * TAU - 1. / DELTA**2)
      SUMX = SUMX * E
      SUM = SUM + SUMX
      IF (1.E-4 * ABS(SUM).GT.ABS(SUMX)) GO TO 900
899   CONTINUE
900   E = ABS(SUM)
C     ***************************************
C
C     COMPUTE RECEIVED POWER IN DBW
C
C     ***************************************
      IF (LAMBDA.LE.0.) LAMBDA = 1.
      IF (E.LT.0.) E = 1.
      IF (PWR.LT.0.) PWR = 1.
      RECPWR = -158.513 + 20. * LOG10(LAMBDA) + 20. * LOG10(E) +
     1 10. * LOG10(PWR)
C     ***************************************
C
C     OUTPUT SECTION
C
C     ***************************************
      SIGMA = SIGMA * 1.E11
      WRITE(2,1000) E,RECPWR,PWR,LAMBDA,D,HT,NPOL,EPSLN,SIGMA
1000  FORMAT (/,1X,'OUTPUT:',///,1X,'FIELD STRENGTH AT R = ',4X,
     11PE9.3,1X,'MICROVOLTS/METER',//,1X,'POWER AT R = ',7X,0PF10.2
     2,6X,'DBW',///,1X,'**************************',///,1X,'INPUT:',
     3///,1X,'T POWER = ',11X,F9.3,6X,'KILOWATTS',
     4//,1X,'WAVELENGTH = ',8X,F9.3,6X,'METERS',//,1X,'DISTANCE
     5 T:R = ',7X,F8.3,6X,'KILOMETERS',//,1X,'HEIGHT OF T = ',7X
     6,F7.1,8X,'METERS',//,1X,'HEIGHT OF R =',8X,F7.1,8X,'METERS',
     7//,1X,'POLARIZATION = ',10X,I1,T38,'0 = VERTICAL, 1 =
     8 HORIZONTAL',//,1X,'EPSILON = ',14X,F5.2,//,1X,'SIGMA = ',17
     9X,1PE8.2,3X,'MHOS/METER')
      END
```

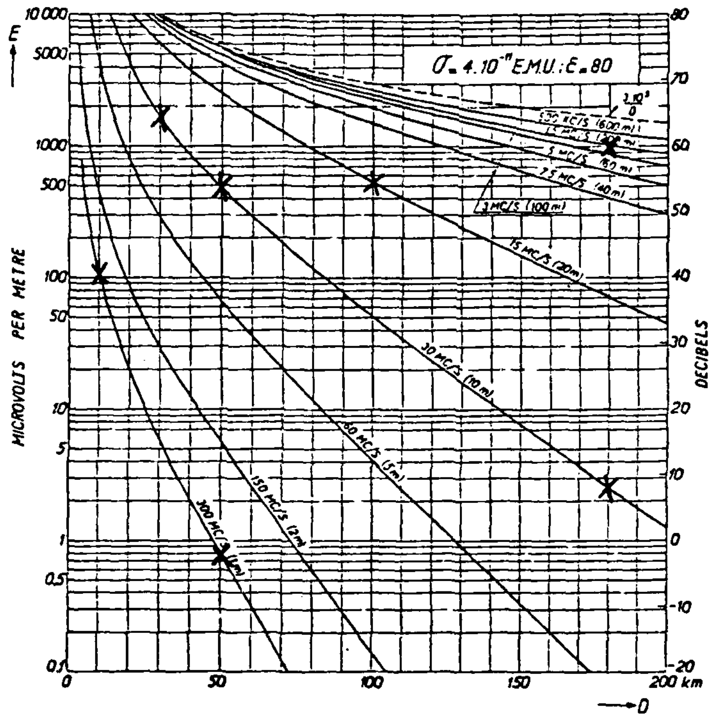

Figure 1. Comparison of ground wave r.m.s. field strengths calculated by the NRC ground wave program (x) and by H. Bremmer.[1] The ground constants apply to sea water, the polarization is vertical, the transmitter power is 1 kw, and both transmitter and receiver are on the ground.

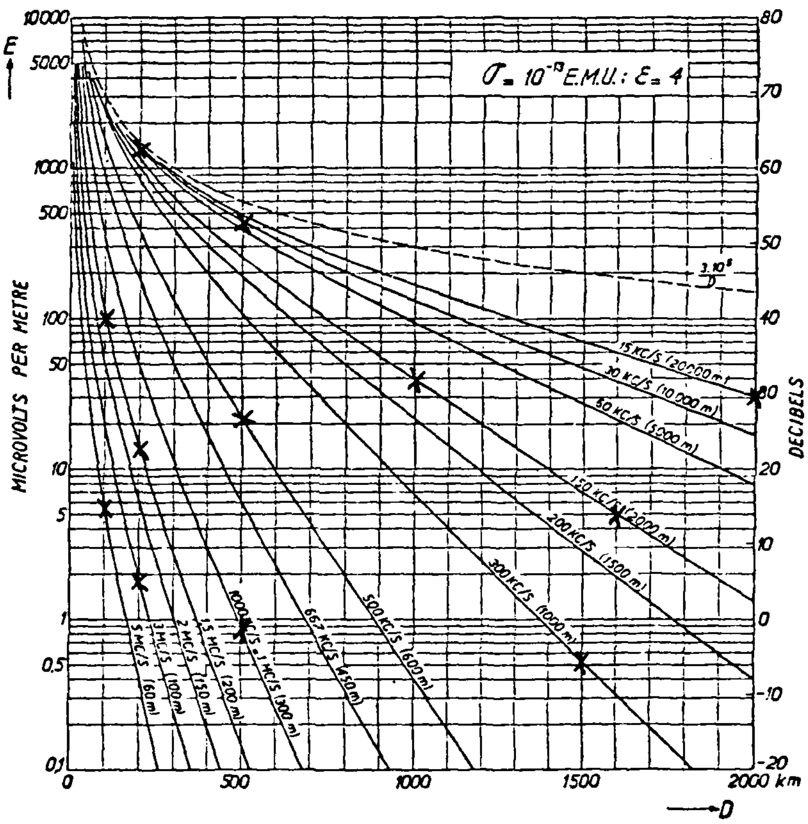

Figure 2. Same as Figure 1 except for average ground.

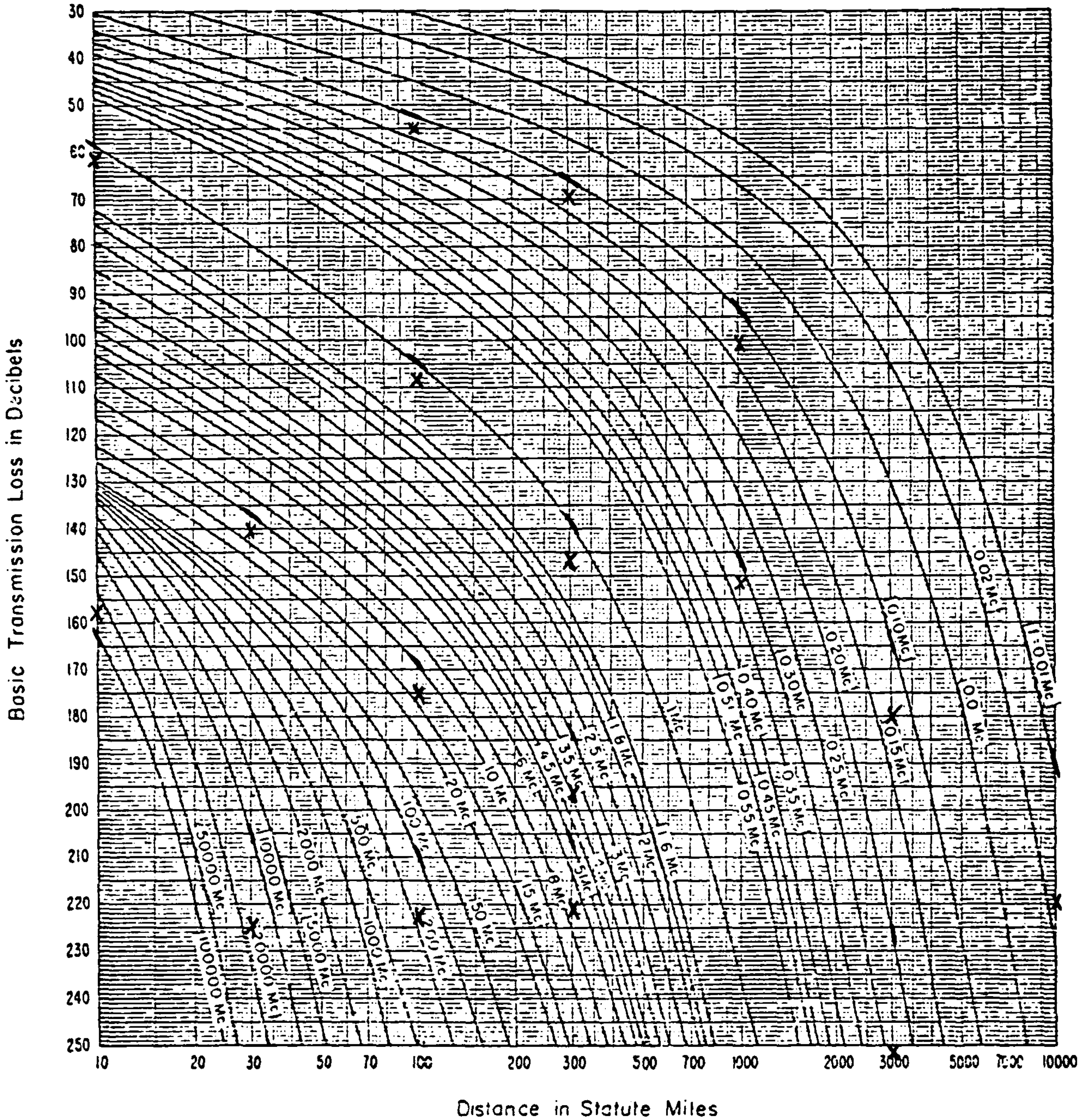

Figure 3. Comparison of basic transmission loss in dB calculated by the MRC ground wave program (x) and by K. Norton.[12] The computations are for average land (σ = .005 mhos/meter, ϵ = 15), vertical polarization and both transmitting and receiving antennas nine meters above the ground.

accomplished with an earlier version of the program using Bremmer's original conventions for transmitter power and distance between transmitter and receiver, not the CCIR conventions now used.) Figures 1 and 2 show that the MRC ground wave program matches Bremmer's computations almost perfectly. The very small differences are probably due to the greater accuracy possible with a computer. (All of Bremmer's results were computed by hand.) In contrast, the comparisons in Figure 3 between MRC and Norton[12] reveal small although significant discrepancies. MRC's results are consistently lower than Norton's. These discrepancies probably arise because Norton also considers atmospheric refraction while we do not. Refraction is discussed further in Section 4.

The MRC results also match the world standard CCIR results from the Geneva conference of 1974,[13] but are somewhat lower than the CCIR results from the Kyoto conference of 1978.[14] This is not surprising because the 1974 results were based on Bremmer's equations while the 1978 results were based on Bremmer's equations but also included refraction. A set of CCIR ground wave propagation curves is provided for reference in the appendix.

The approach used by the MRC program is quite similar to that used by the NUCOM/BREM program.[15]

Using computations from the MRC ground wave program, the curves in Figures 4, 5, and 6 were generated. These curves apply to a 1 kW transmitter and to wide variety of circumstances from sea water to average land, from a frequency of 15 KHz to 10 GHz, from a range of 2 km to 2000 km, and from a receiver height of 0 m to 1000 m. They demonstrate the versatility of the program while not attempting to cover all possible parametric variations. Figure 6 also shows that the program fails to compute correct values for a high receiver height and short distance between transmitter and receiver. The departures from a smooth curve at

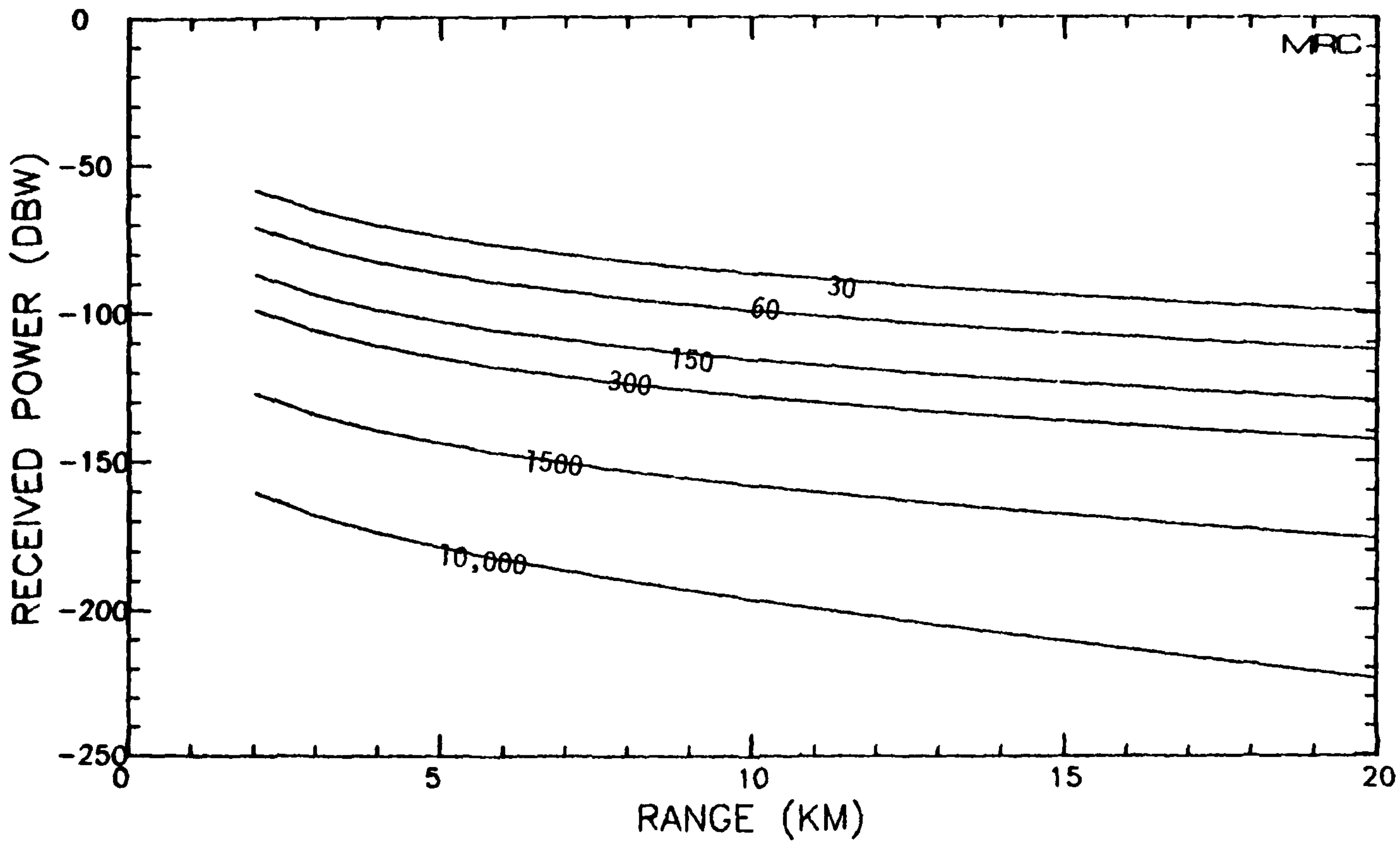

Figure 4. Sample MRC results for ground wave propagation over sea water at various frequencies in MHz. Both the transmitter and receiver are assumed to be at zero elevation and both antennas are vertically polarized.

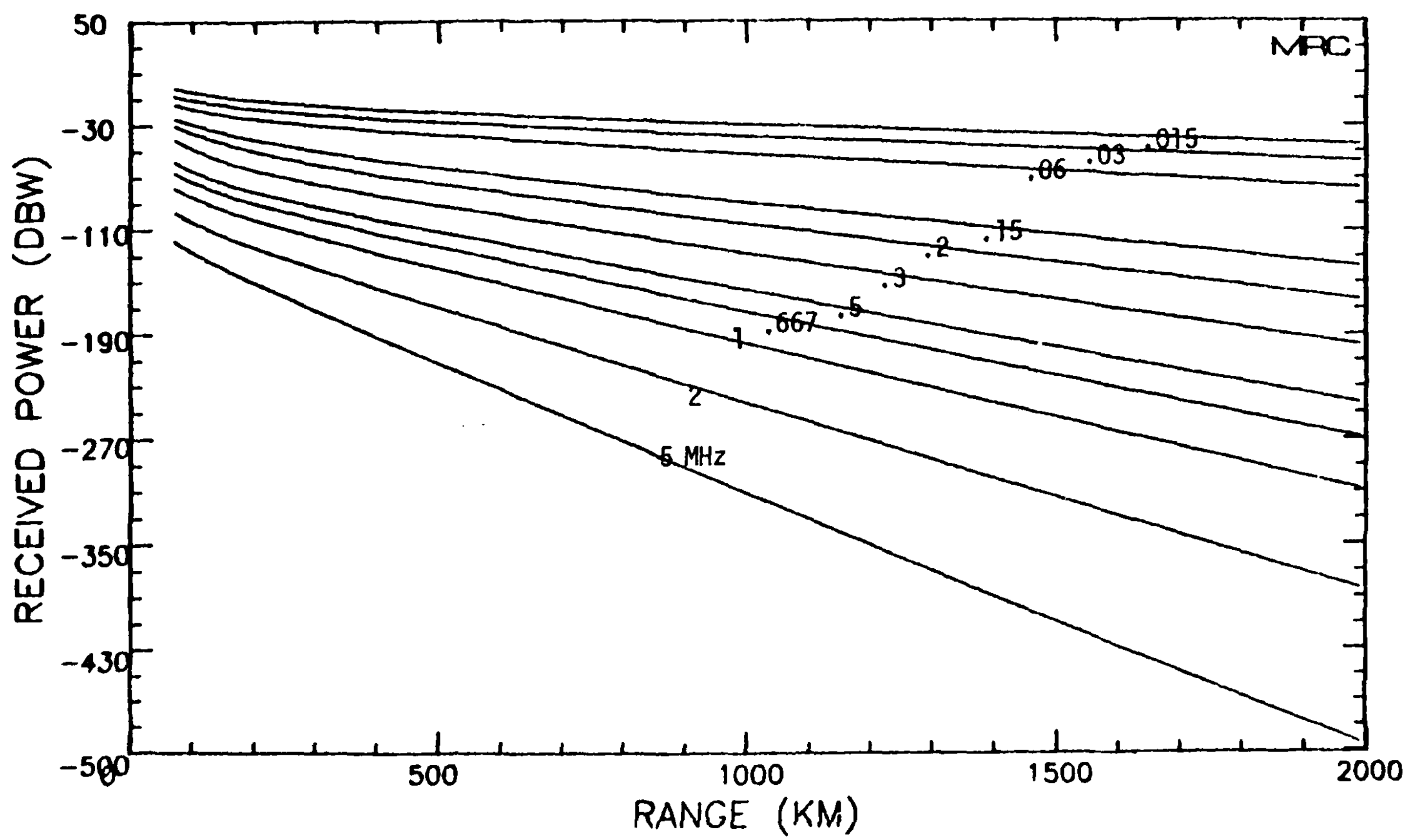

Figure 5. Same as Figure 4 except for average ground.

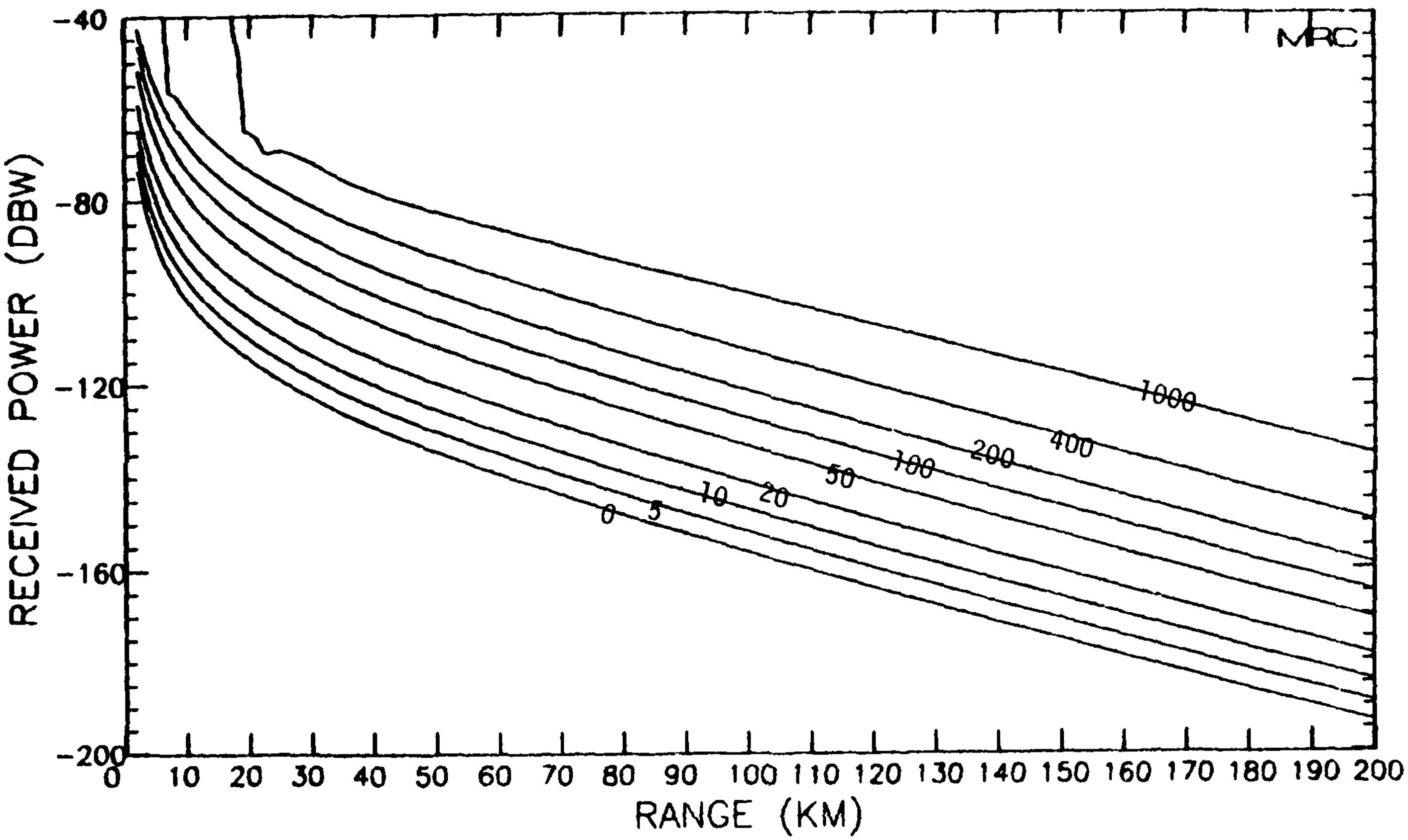

Figure 6. Similar to Figures 4 and 5 except the frequency here is fixed at 30 MHz and the height of the receiver (in m) is varied. The transmitter height is fixed at 10 m and the curves apply to average ground.

receiver heights of 400 and 1000 m are errors. The program generally fails at very short separations between transmitter and receiver. In these cases, a line-of-sight or geometric optical model is more appropriate.

Figures 7 and 8 show one application of the MRC ground wave program to a hypothetical ground wave system. The ground constants used are appropriate to average ground in Germany while the transmitter characteristics used are typical of many commercially available products. The maximum range is determined by the noise level at the receiver and not the receiver itself. Two curves are shown in each figure corresponding to a best and worst case noise. The actual situation will probably be somewhere in between the two extremes. Figure 8 shows the considerable improvement in range that is possible with nominal improvements in transmitter characteristics.

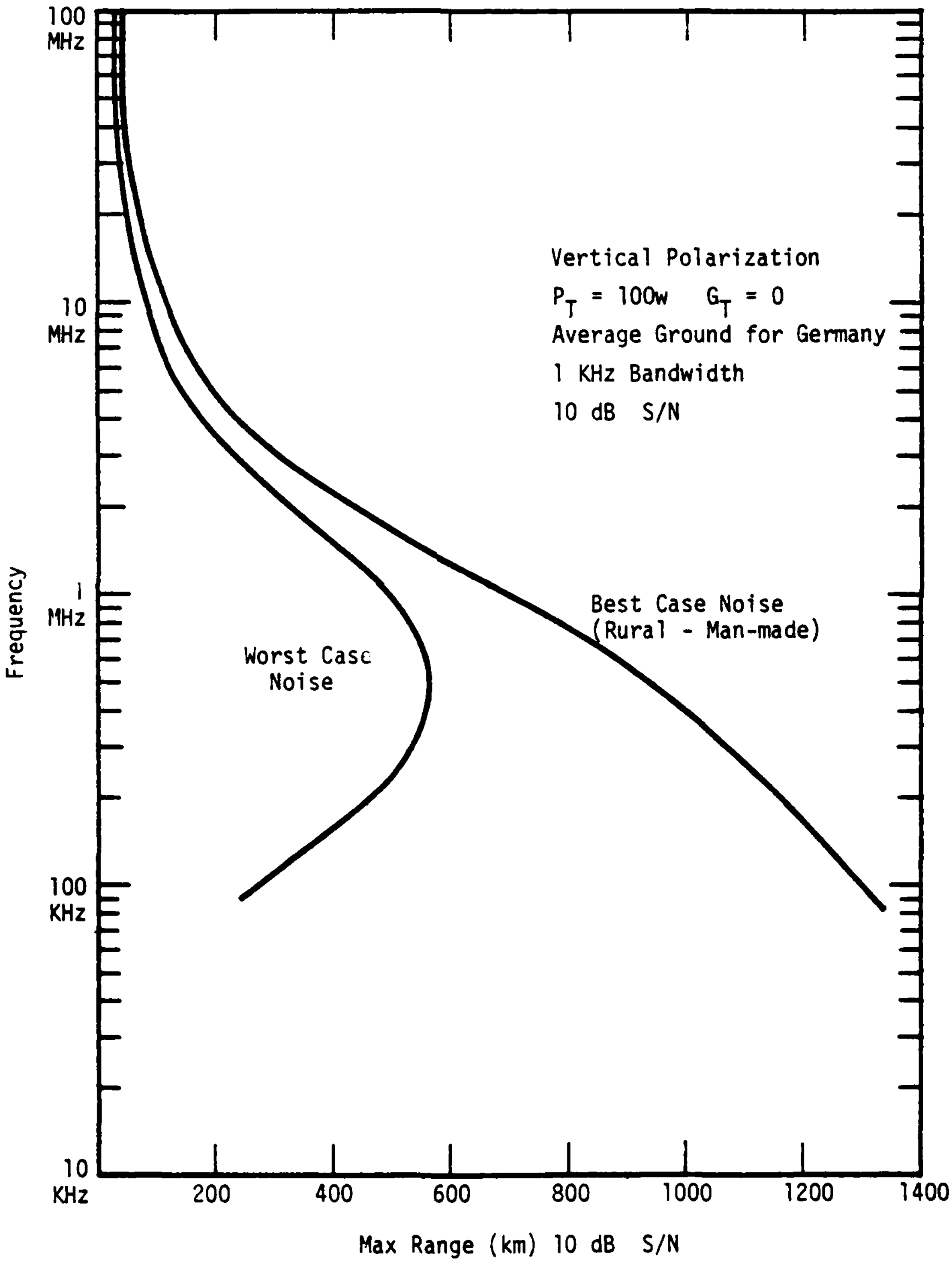

Figure 7. Maximum ground wave range for a hypothetical system in Germany.

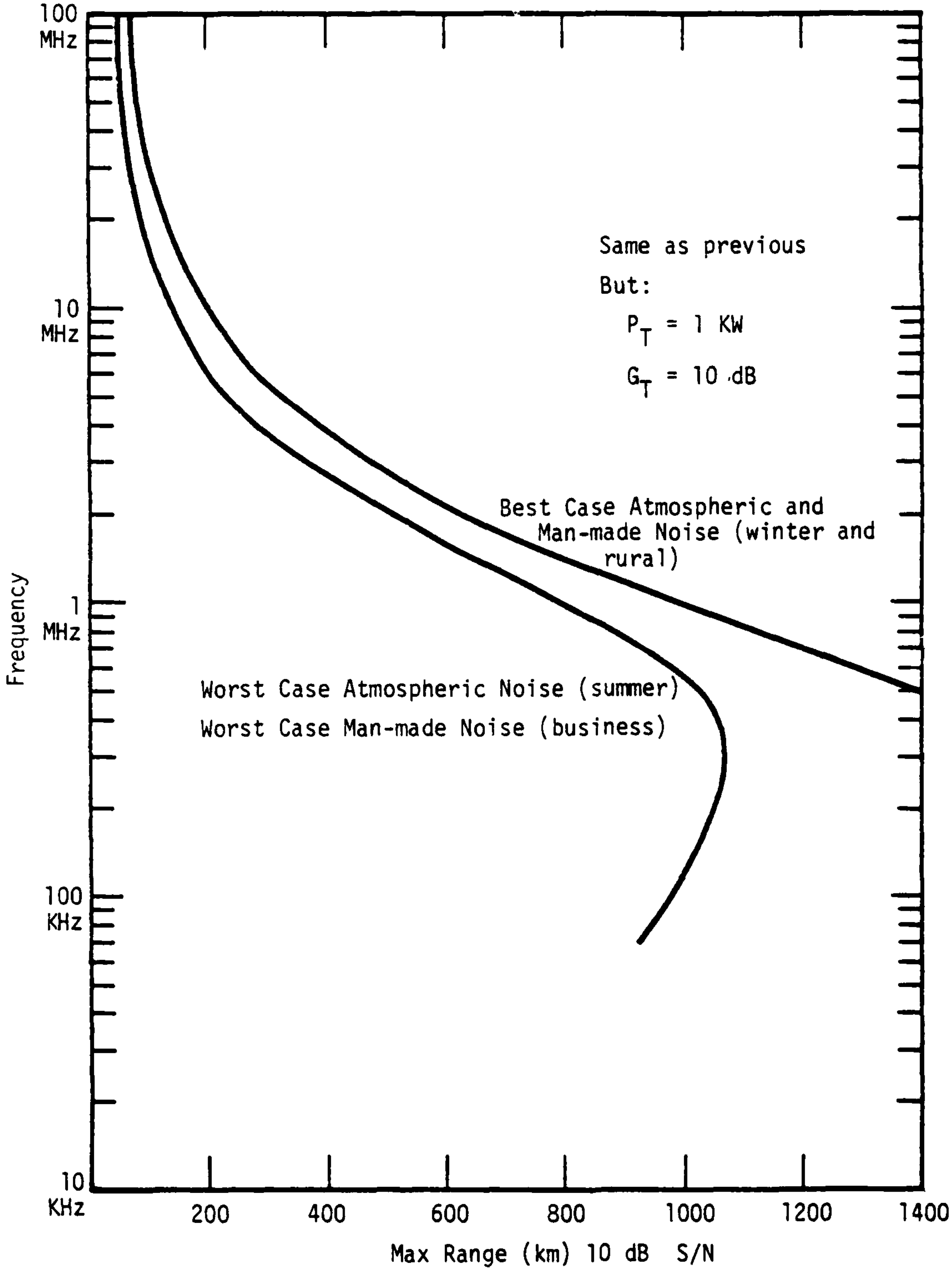

Figure 8. Same as Figure 7 except for improved transmitter characteristics.

SECTION 4
REFRACTION

This section discusses the refraction of ground waves by a non-uniform atmosphere. Figure 9 shows that refraction is a significant effect which, under most but not all circumstances, improves ground wave propagation.

The variation of refractive index as a function of altitude can be expressed in several ways. The following equations show two possibilities

$$\mu(h) = 1 + A \exp(-Bh) \tag{19}$$

and

$$\mu(r) = \sqrt{1-\eta + \gamma \frac{a^2}{r^2}} \tag{20}$$

where A and B as well as η and γ are arbitrary constants chosen to suit the particular location involved. h is the height above mean sea level, r is the distance from the center of the earth, and a is the radius of the earth. Equation 19 comes from the CCIR[14] while Equation 20 comes from Bremmer.[1] Although 19 is now considered the preferable form, 20 is adequate in the lower atmosphere. We choose to use Equation 20 because Bremmer's equations for refraction readily follow from this equation.

Introducing the parameter α,

$$\alpha \equiv \frac{1-\eta}{1-\eta+\gamma} \tag{21}$$

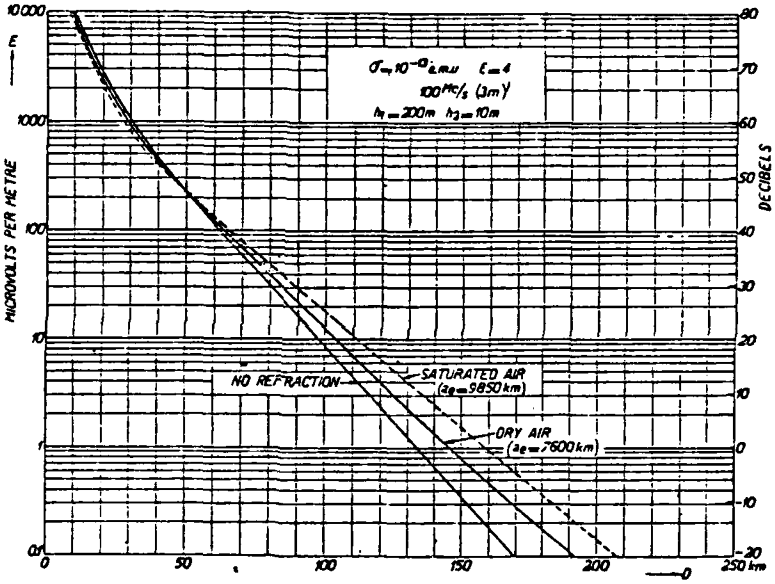

Figure 9. Bremmer's computation of the effect of atmospheric refraction on ground wave r.m.s. field strength.[1] It is interesting to note how the composition of the air changes the refraction.

it can be shown[1] that the electric field E at a distance D and height h_2 from a transmitter at height h_1 over soil with a parameter δ (see Equation 9) can be reduced to the electric field, E_0, that would exist without refraction in the following way:

$$E(D,h_1,h_2,\delta) = \alpha^{2/3} E_0(D\alpha^{2/3}, h_1\alpha^{1/3}, h_2\delta^{1/3}, \delta\alpha^{1/3}) \qquad (22)$$

In other words, Equation 6 can be used to compute the electric field with refraction providing the modified parameters shown in Equation 22 are used. It is also necessary to use the actual wavelength existing at the earth's surface $\lambda_0/\mu(a)$ and not the wavelength in vacuum.

To be able to use Equation 22, it is necessary to evaluate α. This can be done using the following formula for the index of refraction:[1,14]

$$\mu = 1 + 77.6\frac{p}{T} + .373\frac{e}{T^2} \qquad (23)$$

where

T = absolute temperature (°K)

p = atmospheric pressure in millibars

e = water vapor pressure in millibars

Differentiating 20 and 23 with respect to height yields,

$$\mu'(r) = -\frac{\gamma}{a\mu(r)} \qquad (24)$$

and

$$\mu'(h) = -77.6\times10^{-6}\frac{p}{T^2}\frac{dT}{dh} + \frac{77.6\times10^{-6}}{T}\frac{dp}{dh} - .746\frac{e}{T^3}\frac{dT}{dh} + \frac{.373}{T^2}\frac{de}{dh} \qquad (25)$$

Equation 25 can be simplified by use of the relation

$$\frac{dp}{dh} + \frac{de}{dh} = -10\ g\rho \tag{26}$$

where the unit of length is chosen to be 100 m and

g = acceleration of gravity in cm/sec^2

ρ = density of air in g/cm^2.

Substituting Equation 26 in 25 yields

$$\mu'(h) = -\frac{.76}{T}\rho + \left(-77.6\times10^{-6} + \frac{.373}{T}\right)\frac{1}{T}\frac{de}{dh} \tag{27}$$

$$- \left(77.6\times10^{-6}\ p + .746\ \frac{e}{T}\right)\frac{1}{T^2}\ \frac{dT}{dh}$$

Because refraction takes place close to the earth's surface, $\mu(r)$ and $\mu'(r)$ can be adequately approximated by conditions at the earth's surface. Because

$$\gamma-\eta = \mu^2(a)-1 \approx .00058 \approx 0 \tag{28}$$

$\gamma-\eta$ can be neglected. Then (24) can be written

$$\mu'(a) = -\frac{\eta}{a} \tag{29}$$

Equations 21, 27, and 29 can be combined to provide the following solution for α in terms of atmospheric conditions near the earth's surface

$$\alpha \approx 1 - a\left[\frac{.76}{T}\rho + \left(77.6\times10^{-6} + \frac{.373}{T}\right)\frac{1}{T}\frac{de}{dh}\right. \tag{30}$$

$$\left. + \left(77.6\times10^{-6}\ p + .746\ \frac{e}{T}\right)\frac{1}{T^2}\frac{dT}{dh}\right]$$

Equation 30 when used in conjunction with Equation 22 is an adequate formal solution of the refraction problem which can be readily adapted for use on a computer. Using a better approximation than Equation 29 will lead to a slightly better solution of the refraction problem.

Without a computer, the formal solution of Equations 22 and 30 can still be used by employing several additional approximations. Using the approximation in Equation 28, Equation 22 can be rewritten

$$E(D,h_1,h_2) = (1-\eta)^{4/3} E_0[D(1-\eta)^{2/3}, h_1(1-\eta)^{1/3}, h_2(1-\eta)^{1/3}] \quad (31)$$

This equation further assumes that δ (given in Equation 9) is small. That is,

$$|\delta| = K \ll 1 \quad . \quad (32)$$

This occurs for short wavelengths from VHF and shorter (perhaps also for portions of the HF band depending on the ground constants used). In any case, Equation 31 is considerably simpler than 22.

Without refraction the electric field depends on D principly thru the parameter, χ, given in Equation 7:

$$\chi = (2\pi)^{1/3} D/(a^{2/3} \lambda^{1/3}) = .053693\ D_{km}/\lambda_m{}^{1/3} \quad (33)$$

From this expression, it is evident that changing D to $D(1-\eta)^{2/3}$ is equivalent to changing the radius of the earth to $a/(1-\eta)$ and holding D constant. The effective radius of the earth can then be written

$$a_e = a / [.766 - (.0681 + .00237\ e) \frac{dT}{dh} + .306 \frac{de}{dh}] \quad (34)$$

using Equations 27 and 29 and evaluating T and p at standard temperature and pressure (STP).

Equation 34 is a most interesting expression. It is evident that for a dry atmosphere with an adiabatic temperature gradient ($dT/dh \approx -1$), $a_e \approx 1.20a$. For saturated air, $a_e \approx 1.55a$. For mean meteorological conditions $a_e \approx (4/3)a$, which is an often used value. Under some conditions $a_e < a$, and the refraction will actually hinder ground wave propagation. In contrast, a temperature inversion ($dt/dh > 0$) will considerably enhance radio propagation.

To compute the resulting electric field in the case of refraction using the approximations above, it is only necessary to take a graph of E versus D without refraction and multiply E by $(1-\eta)^{4/3}$ and D by $1/(1-\eta)^{2/3}$. If h_1 and h_2 are non zero, then they must be similarly reduced as shown in Equation 31. The graph in Figure 9 was prepared by Reference 1 using this technique.

SECTION 5
PROPAGATION OVER IRREGULAR TERRAIN

Up to this point, we have assumed that the earth is a smooth homogeneous sphere. Although the earth varies substantially from this idealization, the results expressed in Equation 6 are applicable to many situations. Nevertheless, it would be useful to compute field strengths for those cases where Equation 6 is clearly not valid. For instance, propagation over mountains or propagation from land to ocean is not well described by Equation 6. The literature on these subjects is extensive and well beyond the scope of this paper. We arbitrarily choose to discuss propagation over obstacles and to refer the reader to other work for discussions of propagation over inhomogeneous or inductive terrain. In all of these cases, the results occasionally differ from simple intuitive extensions of Equation 6 because of the unusual nature of diffraction processes. For instance, a large obstacle between a transmitter and receiver can actually increase the received signal strength. Such an effect is called "obstacle gain" and is explained below.

Propagation over inhomogeneous terrain can be handled in various ways. The Suda method[16] involves averaging the ground constants for various segments of the terrain while the Millington method[17,18] involves a geometrical mean of the electric fields due to the various segments. The Suda method is most appropriate where the ground constants do not change substantially while the Millington method is applicable to substantial changes as long as the field is measured well away from the interface region. Many other references have considered these approaches as well as others. References 15 and 19 through 31 discuss the subject in detail. In addition, Reference 32 discusses propagation over inductive terrain.

Propagation over obstacles has also been covered extensively in the literature. The problem can be expressed in a formal manner in terms of a two dimensional integral equation of the following type:[11,33]

$$W(p) = 1 - \frac{1}{2\pi} \iint W(Q)\, e^{ik_0(TQ + QP - PT)} \frac{TP}{QP \times QT} \times \left[\gamma(Q) - \left(ik_0 - \frac{1}{QP}\right) \frac{\partial QP}{\partial n_Q}\right] dO \quad . \tag{35}$$

W is the ratio of the actual amplitude of the Hertzian vector to its value for the case of a perfectly conducting plane earth. The distances TQ, QP, etc. are indicated in Figure 10. The function γ is related to the tilt of the field as well as to so-called surface admittances. The integral extends over the entire irregular portion of the earth's surface except for an infinitesimal area around P. This equation can account for both irregular and inhomogeneous terrain.

Equation 35 can be reduced to a one-dimensional equation provided that the irregular surface of the earth does not deviate too greatly from an average level plane or that the various ground parameters do not vary too greatly perpendicular to the line connecting the transmitter, T, and receiver, P. A saddlepoint approximation simplifies 35 to

$$W_1(x) = 1 - \sqrt{\frac{ix}{2\pi k_0}} \int_0^x \frac{W_1(\xi)}{\sqrt{\xi(x-\xi)}} \left[\gamma_1(\xi) + ik_0 \sin \alpha_1(\xi)\right] e^{ik_0(TQ+QP-PT)} d\xi \tag{36}$$

This expression shows that:

a) Local changes of the ground constants and of the terrain profile have a similar effect on W_1. The term in square

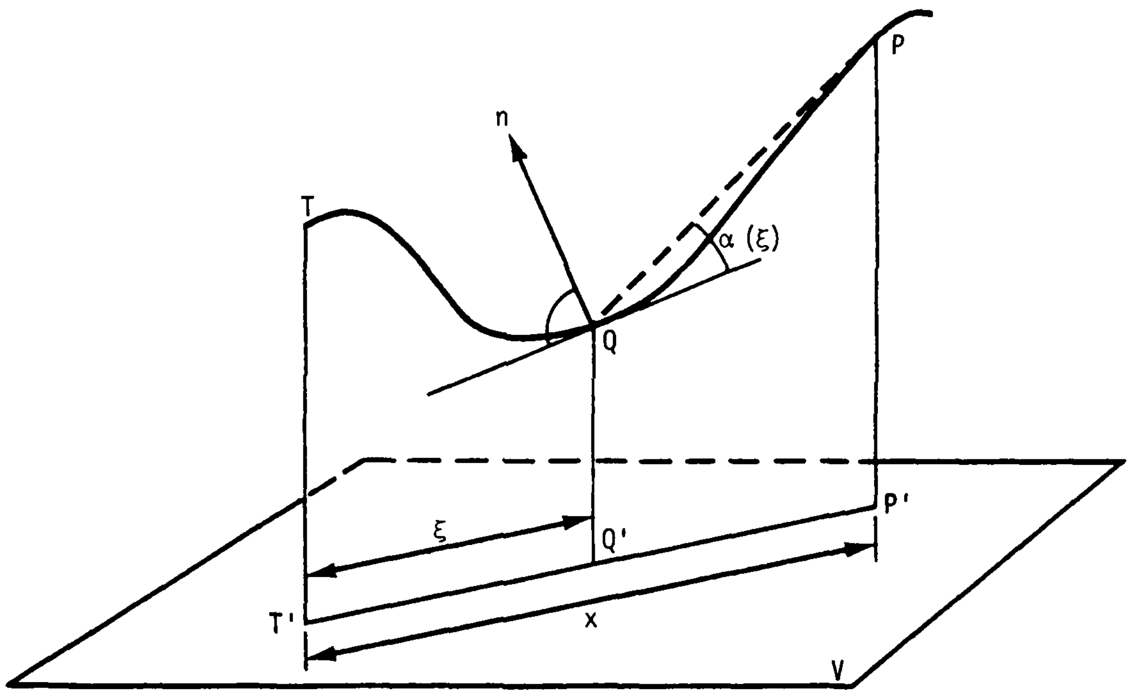

Figure 10. Geometrical representation of an irregular terrain profile.

brackets shows that γ, representing ground constants, and α, representing terrain profile, have a similar effect.

b) The terrain near the transmitter and receiver has a relatively greater influence due to the existence of the weighting factor $1/\sqrt{\xi(x-\xi)}$.

It is possible to reduce Equation 35 to Equation 36 because of the dominating role of integration points, Q, near stationary values of an exponential phase factor. The region surrounding the area of a stationary phase is the first Fresnel zone. Figure 11 shows a drawing of this zone. Terrain irregularities and inhomogeneities produce significantly different results if they occur inside or outside this first Fresnel zone. Inside the zone, disturbances can prevent production of the main field at the receiver. This is the field that would have occurred had no disturbances been present. In contrast, disturbances outside the zone will not significantly alter the main field but may add some perturbations. If the transmitter and/or receiver are elevated, the same reasoning applies but the first Fresnel zone is somewhat different.

Major obstacles between the transmitter and receiver, such as the ridge shown in Figure 12, can produce a surprising result known as "obstacle gain". The ridge is assumed to be within the first Fresnel zone and well above the shortest path between the transmitter and receiver. In this case, the ridge acts approximately like the absorbing straight edge often considered in the theory of optical diffraction.[2] The field at or beyond the ridge can be estimated from the Cornu spiral shown in Figure 13. The starting point for the spiral is fixed at the lower point of the spiral, and the various chords, a through g, correspond to the magnitude and phase of the electric field. Only the end point of the chord changes with x. (x is the coordinate perpendicular to the straight edge and

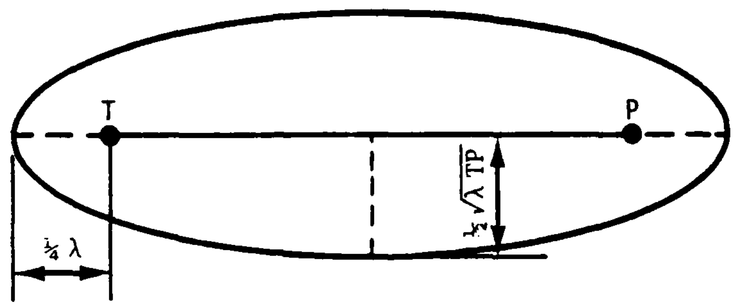

Figure 11. First Fresnel zone for propagation along the earth. The transmitter T and receiver P are on the earth.

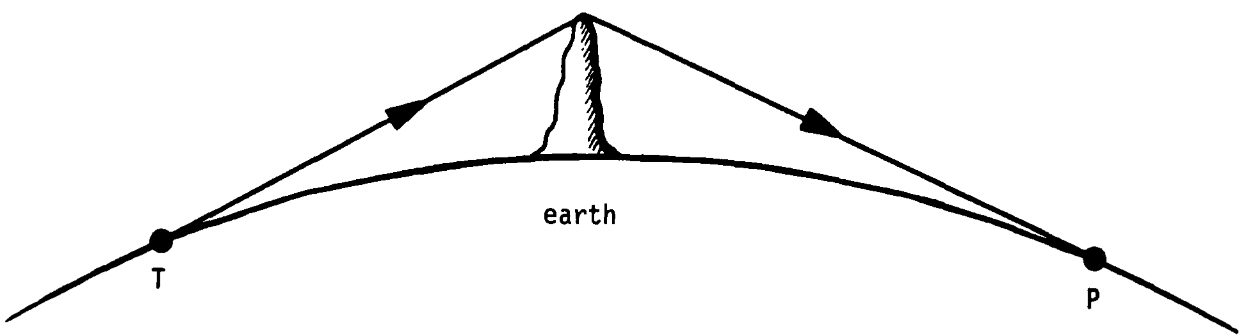

Figure 12. Propagation utilizing a ridge to produce "obstacle gain".

parallel to the wave front.) In the geometrical shadow region ($-\infty < x < 0$) the length of the chord increases steadily as indicated by points a through d. d corresponds to the boundary of the shadow region. From this point, the chord keeps increasing in length until it reaches a maximum at f and then begins an oscillatory behaviour approaching the other end of the sprial. Figure 14 shows this effect explicitly.

Behind the diffracting straight edge the field is given approximately by

$$u = \frac{(1+i)}{4\sqrt{\pi kr}} e^{ikr} \left[\frac{1}{\cos\left(\frac{\phi-\alpha}{2}\right)} \mp \frac{1}{\cos\left(\frac{\phi+\alpha}{2}\right)} \right] \tag{37}$$

where u represents the electric field when it is parallel to the edge and the minus sign applies. When the electric field is perpendicular to the edge, u represents the magnetic field and the plus sign applies. Equation 37 assumes a cylindrical coordinate system with the z-axis parallel to the straight edge and the angular coordinate $\phi=0$ or 2π at the straight edge. α is the angle between the wave normal and straight edge. Because the value in square brackets decreases slowly with increasing ϕ, the light or radio wave is diffracted far into the shadow region. Equation 37 is based on an approximation which fails at the shadow boundary $\phi = \alpha$ or $\phi = -\alpha$.

Equation 37 shows that the diffracted field beyond the ridge falls off as $r^{-1/2}$. This is less of a decrease than for ground wave propagation over a flat earth (r^{-2}) or a curved earth (e^{-r/r_0}). In front of the ridge, the field decreases as r^{-1} which is also better than ground wave propagation. In other words, a sharp ridge can actually improve reception at a distant location behind the ridge. Because typical soil conditions produce considerable absorption of ground waves while a propagation path over a high ridge avoids the ground to a large extent, improved propagation is possible by utilizing a ridge.

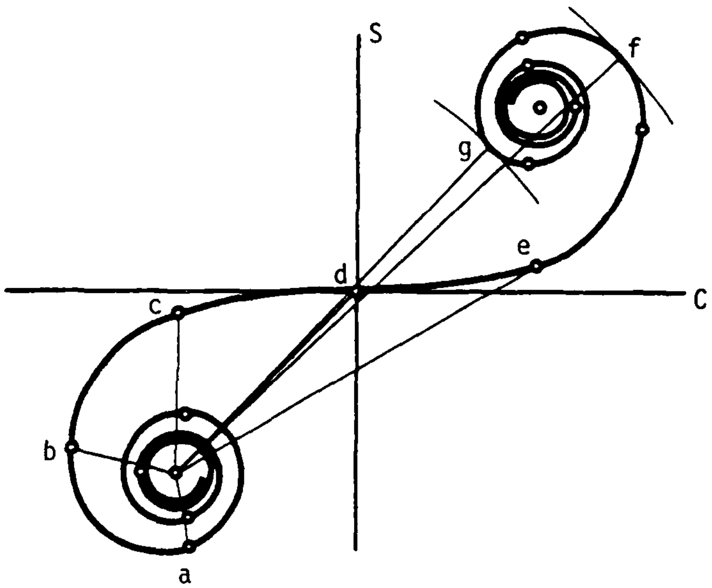

Figure 13. Cornu spiral construction for determining the diffraction pattern produced by a straight edge. The axes labeled S and C represent the Fresnel integrals.

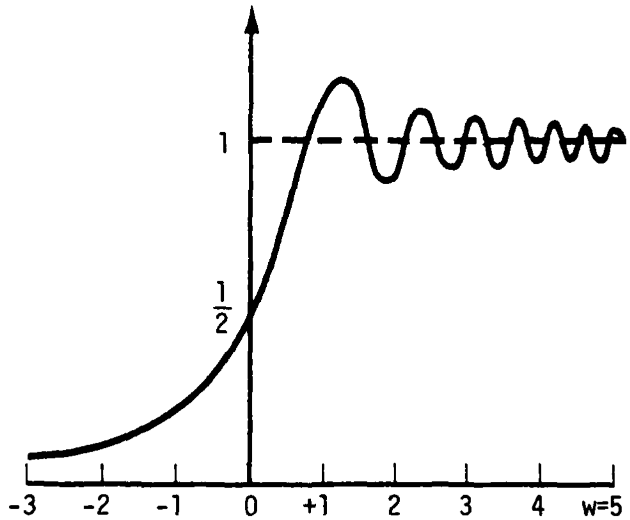

Figure 14. Amplitude of the electric field at a straight edge. Zero corresponds to the boundary of the edge, negative values of w are behind the edge while positive are in front of the edge.

Several computer programs have been developed to compute ground wave propagation over irregular and inhomogeneous terrain. These require a detailed knowledge of the terrain between the transmitter and receiver and involve long or short wavelength approximations. One program developed by the Communications Research Centre[34] applies to frequencies at VHF or higher. Another, developed by ITS[35] applies to MF and lower frequencies but can be stretched into the HF. The basic difficulty with the HF is that the radio wavelength is close to the size of terrain features so that both long and short wavelength approximations have limited applicability.

Another difficulty in the HF band is the decided lack of experimental data to help verify computer routines. While ground wave data for rough terrain exists at MF and VHF, it is surprising that little exists at HF. Perhaps the HF has been ignored because it is used principly for longer distance sky wave propagation. In any case, data at HF is essential to further our ability to accurately predict HF propagation over rough terrain.

Several investigators have collected data over rough terrain at frequencies outside the HF.[35-40] Of these the work by ITS is perhaps the most thorough.[35,36] This data has been used to show that the ITS program called WAGNER is indeed able to predict ground wave propagation over rough terrain below a few megahertz.

REFERENCES

1. Bremmer, H., Terrestrial Radio Waves/Theory of Propagation, Elsevier Publishing Company, Inc., New York, 1949.

2. Sommerfeld, A., Optics, Academic Press, 1964.

3. Sommerfeld, A., "Ueber die Ausbreitung der Wellen in der Drahtlosen Telegraphie," Ann. Phys. Lpz., 28, 1909.

4. Watson, G.N., "The Diffraction of Radio Waves by the Earth," Proc. Roy. Soc., A95, 1918.

5. Van der Pol, B., and H. Bremmer, "The Diffraction of Electromagnetic Waves from an Electric Point Source Round a Finitely Conducting Spherical Earth," Phil. Mag., 7, 24, 1937.

6. Van der Pol, B., and H. Bremmer, "The Propagation of Radio Waves Over a Finitely Conducting Spherical Earth," Phil. Mag., 7, 25, 1938.

7. Van der Pol, B., and H. Bremmer, "Further Note on the Propagation of Radio Waves Over a Finitely Conducting Spherical Earth," Phil. Mag. 7, 27, 1939.

8. Norton, K.A., "The Propagation of Radio Waves over the Surface of the Earth and in the Upper Atmosphere," Proc IRE, 25, 9, 1937.

9. Norton, K.A., "The Physical Reality of Space and Surface Waves in the Radiation Field of Radio Antennas," Proc IRE, 25, 9, 1937.

10. Norton, K.A., "The Calculation of Ground-Wave Field Intensity Over a Finitely Conducting Spherical Earth," Proc. IRE, 1941.

11. Bremmer, H., "Propagation of Electromagnetic Waves" in Handbuch Der Physik, S. Flügge, ed., Springer-Verlag, 1958.

12. Norton, K.A., Transmission Loss in Radio Propagation : II, NBS Note 12, June 1959.

13. CCIR, "XIII Plenary Assembly, Propagation in Non-Ionized Media," 5, 1974.

14. CCIR, "Recommendations and Reports of the CCIR, 1978, Propagation in Non-Ionized Media," 5, 1978.

15. Nelson, G.P., NUCOM/BREM: An Improved HF Propagation Code for Ambient and Nuclear Stressed Ionospheric Environments, DNA 4248T, GET Sylvania, October 1976.

16. Suda, K., "Field Strength Calculation," Wireless Engineer, 47, 1956.

17. Millington, G., "Ground Wave Propagation Over an Inhomogeneous Smooth Earth, PIEE, 96, 1949.

18. Millington, G., and G. Isted, "Ground Wave Propagation over an Inhomogeneous Smooth Earth: Part 2," PIEE (London), 97 (III), 1950.

19. Feinberg, E., "On the Propagation of Radio Waves Along an Imperfect Surface," J. Phys, Moscow, 10, 1946.

20. Furutsu, K., "The Calculation of Field Strength over Mixed Paths on a Spherical Earth," J. Radio Res. Labs. (Japan), 3, 1956.

21. Wait, J.R., "Mixed Path Ground Wave Propagation: 1. Short Distances," JNBS, 57, 1959.

22. Wait, J.R. and Householder, J., "Mixed Path Ground Wave Propagation, 2. Larger Distances," JNBS, 65, 1961.

23. Wait, J.R., "The Propagation of Electromagnetic Waves Along the Earth's Surface," in Electromagnetic Waves, R.E. Langer, ed., University of Wisconsin Press, 1962.

24. Anderson, J.B., "Reception of Sky Wave Signals Near a Coastline," JNBS, 67, 1963.

25. Wait, J.R. and K.P. Spies, "Propagation of Radio Waves Past a Coastline with a Gradual Change of Surface Impedence, IEEE, 14, 1964.

26. Wait, J.R., "Electromagnetic Surface Waves," in Advances in Radio Research, 1, J.A. Saxton, ed., Academic Press, 1964.

27. Knight, P., The Influence of the Ground and the Sea on Medium-Frequency Sky Wave Propagation, BBC Research Report RA-25, 1968.

28. Rosich, R.K., Attenuation of High-Frequency Ground Waves over an Inhomogeneous Earth, ITS, OT/ITS RR6, 1970.

29. de Jong, D., "Electromagnetic Wave Propagation over an Inhomogeneous Flat Earth (Two-Dimensional Integral Equation Formulation)," Radio Science, 10, 11, 1975.

30. Bahar, E., "Transient Electromagnetic Response from Irregular Models of the Earth's Surface," Radio Science, 13, 2, 1978.

31. Field, E.C. and R. Allen, Propagation of the Low Frequency Ground Wave over Non-Uniform Terrain, Pacific-Sierra, RADC-TR-78-68, 1978.

32. Hill, D.A. and J.R. Wait, "Ground Wave Attenuation Function for a Spherical Earth with Arbitrary Surface Inpedance," Radio Science, 15, 3, 1980.

33. Hufford, G.A., "An Integral Equation Approach to the Problem of Wave Propagation over an Irregular Terrain," J. Appl. Math., 9, 1952.

34. Palmer, F.H., The CRC VHF/UHF Propagation Prediction Program, CRC, 1979.

35. Ott, R.H., L.E. Vogler, and G.A. Hufford, Ground Wave Propagation Over Irregular, Inhomogeneous Terrain: Comparisions, Calculations and Measurements, NTIA-Report-79-20, May 1979.

36. Kissick, W.A., E.J. Haakinson, and G.H. Stonehocker, Measurements of LF and MF Radio Propagation Over Irregular, Inhomogeneous Terrain, NTIA-Report-78-12, November 1978.

37. Ott, H.R., L.E. Vogler, and G.A. Hufford, "Ground Wave Propagation Over Irregular, Inhomogeneous Terrain: Comparisons of Calculations and Measurements, IEEE Transactions on Antennas and Propagation, AP-27, 2, March 1979.

38. Johnson, M.E., M.J. Miles, P.L. McQuate, and A.P. Barsis, Tabulations of VHF Propagation Data Obtained Over Irregular Terrain at 20, 50, and 100 MHz, Part 1 and 2, ESSA Technical Report-IER38-ITSA38, May 1967.

39. Crombie, D.D., Further HF Tests on the Wyoming Buried Dipole, ESSA, ERLTM-ITS250, 1970.

40. Causebrook, J.H., "Medium-wave Propagation in Built-up Areas," Proc. IEE, 125, 9, 1978.

41. Causebrook, J.H., "Electric/Magnetic Field Ratios of Ground Waves in a Realistic Terrain," Elec. Lett., 14, 19, 1978.

APPENDIX

The following curves, considered to be the best available predictions of ground wave field strengths, are reproduced from the CCIR conference of 1978 in Kyoto, Japan. They come from the corrigendum to volume V, Propagation in Non-Ionized Media, and are dated February 25, 1980.

The curves refer to the following conditions:

a) smooth homogeneous earth
b) transmitter and receiver are on the earth
c) transmitting antenna is an ideal Hertzian vertical electric dipole (nearly identical to a vertical antenna shorter than one quarter wavelength)
d) transmitter power is defined in exactly the same way as indicated in Section 3 (basically 1 kw).
e) refraction is accounted for by assuming an atmosphere in which the refractive index decreases exponentially with height.
f) ionospheric reflections are excluded.
g) distances are measured around the curved surface of the earth.

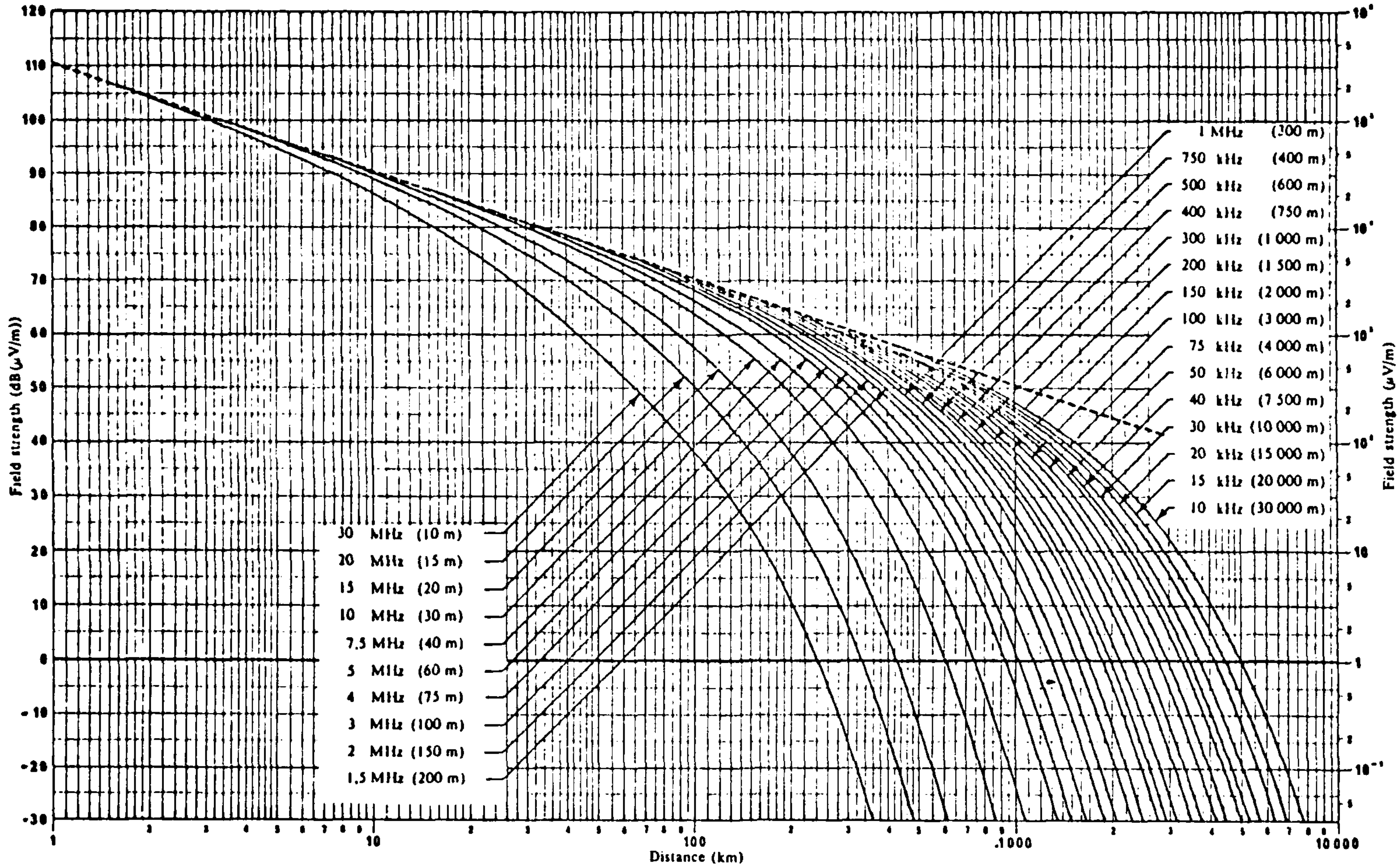

Figure A-1. Ground wave propagation curves; Sea, $\sigma = 5$ S/m, $\epsilon = 80$.

----- Inverse distance curve

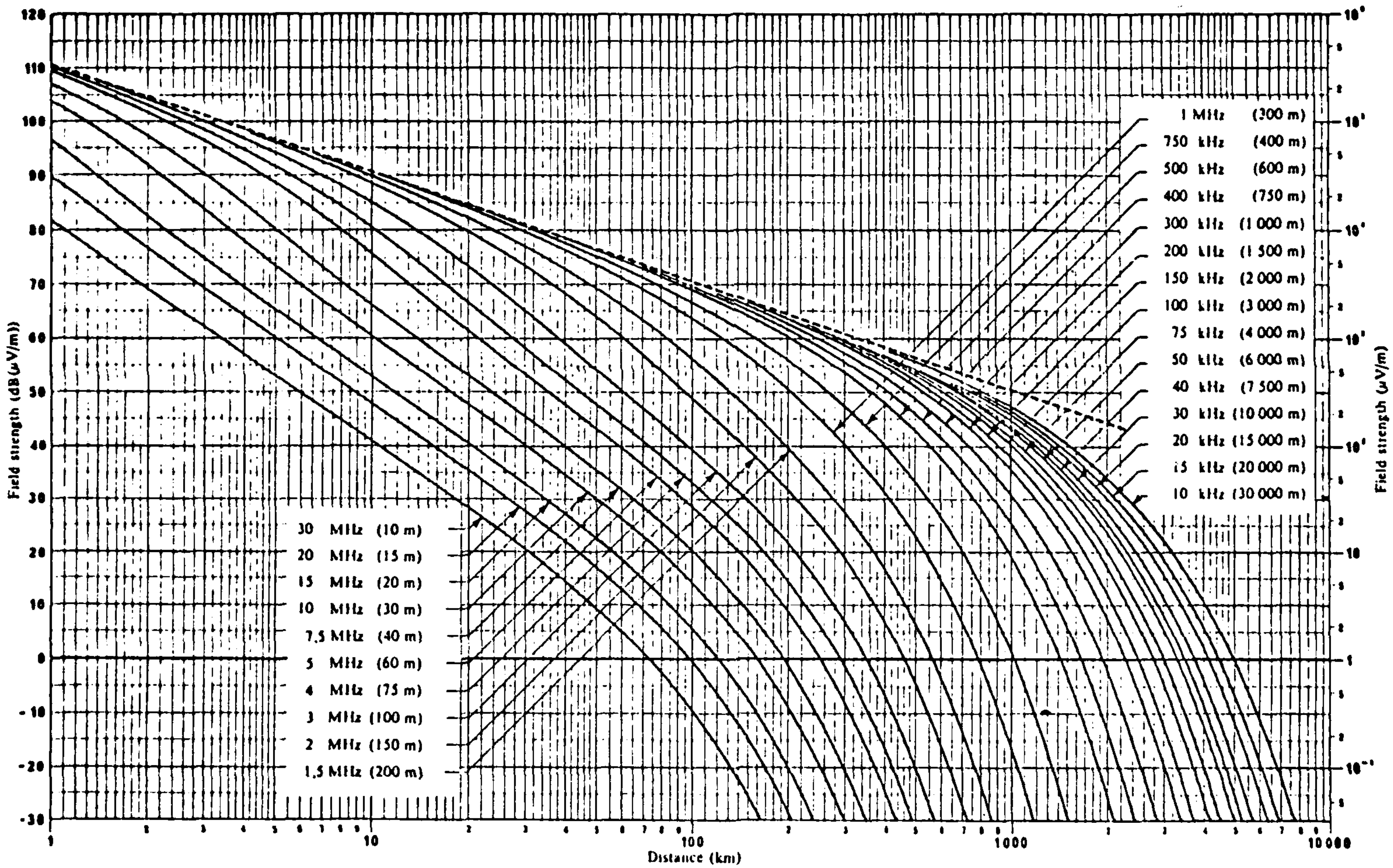

Figure A-2. Ground wave propagation curves; Land, $\sigma = 3 \times 10^{-2}$ S/m, $\epsilon = 4$.

----- Inverse distance curve

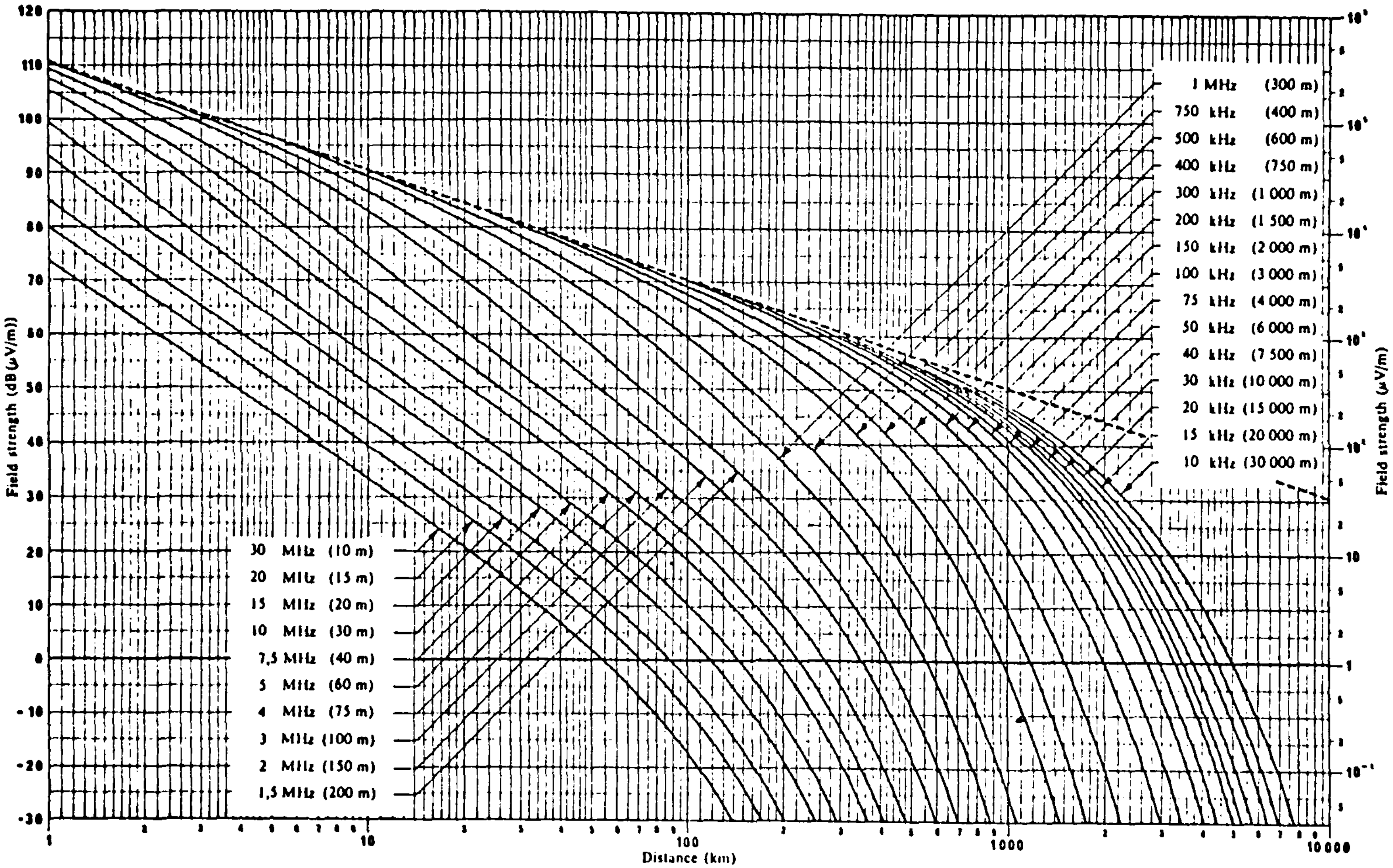

Figure A-3. Ground wave propagation curves; Land, $\sigma = 10^{-2}$ S/m, $\epsilon = 4$.

----- Inverse distance curve

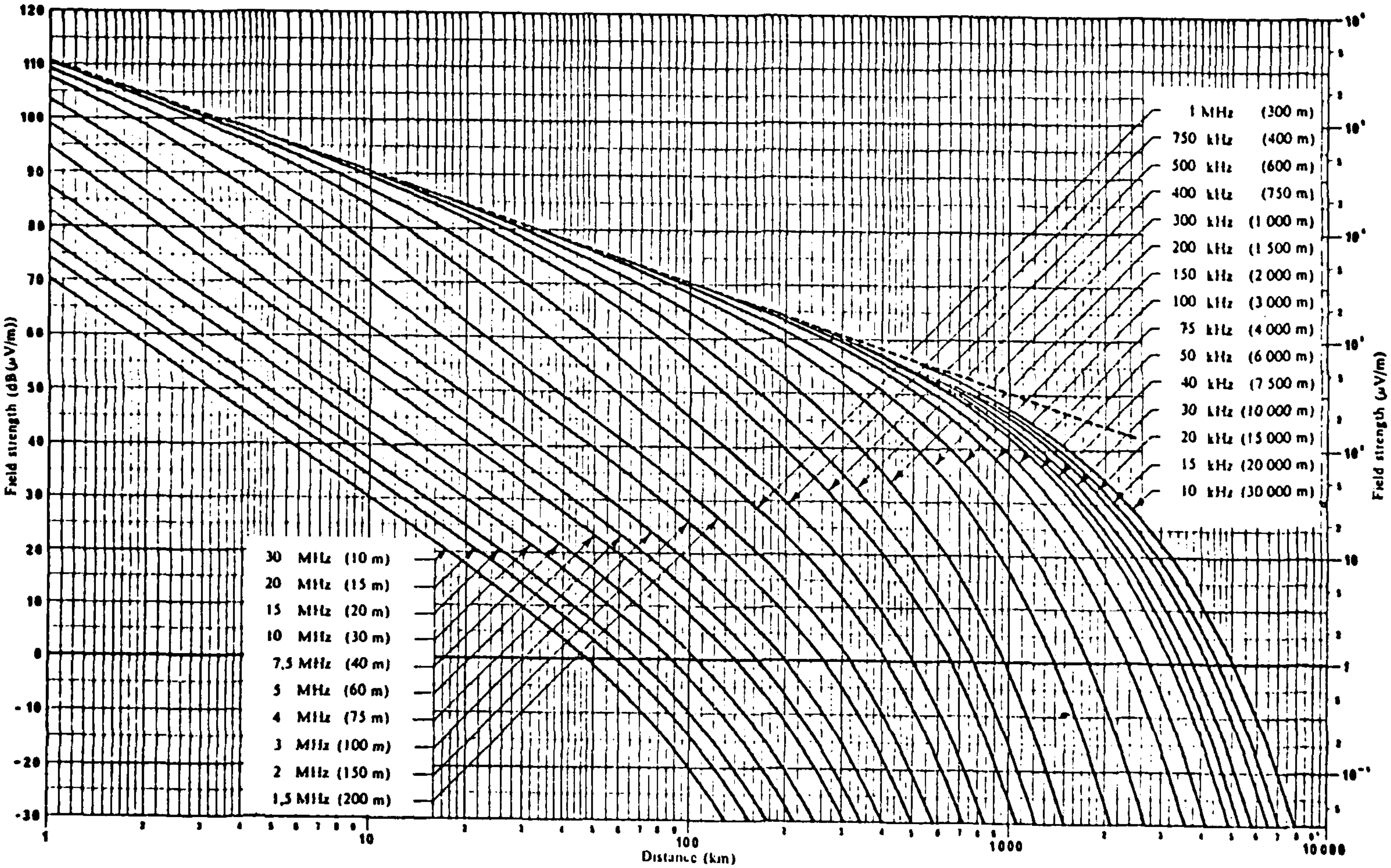

Figure A-4. Ground wave propagation curves; Land, $\sigma = 3 \times 10^{-3}$ S/m, $\varepsilon = 4$.

----- Inverse distance curve

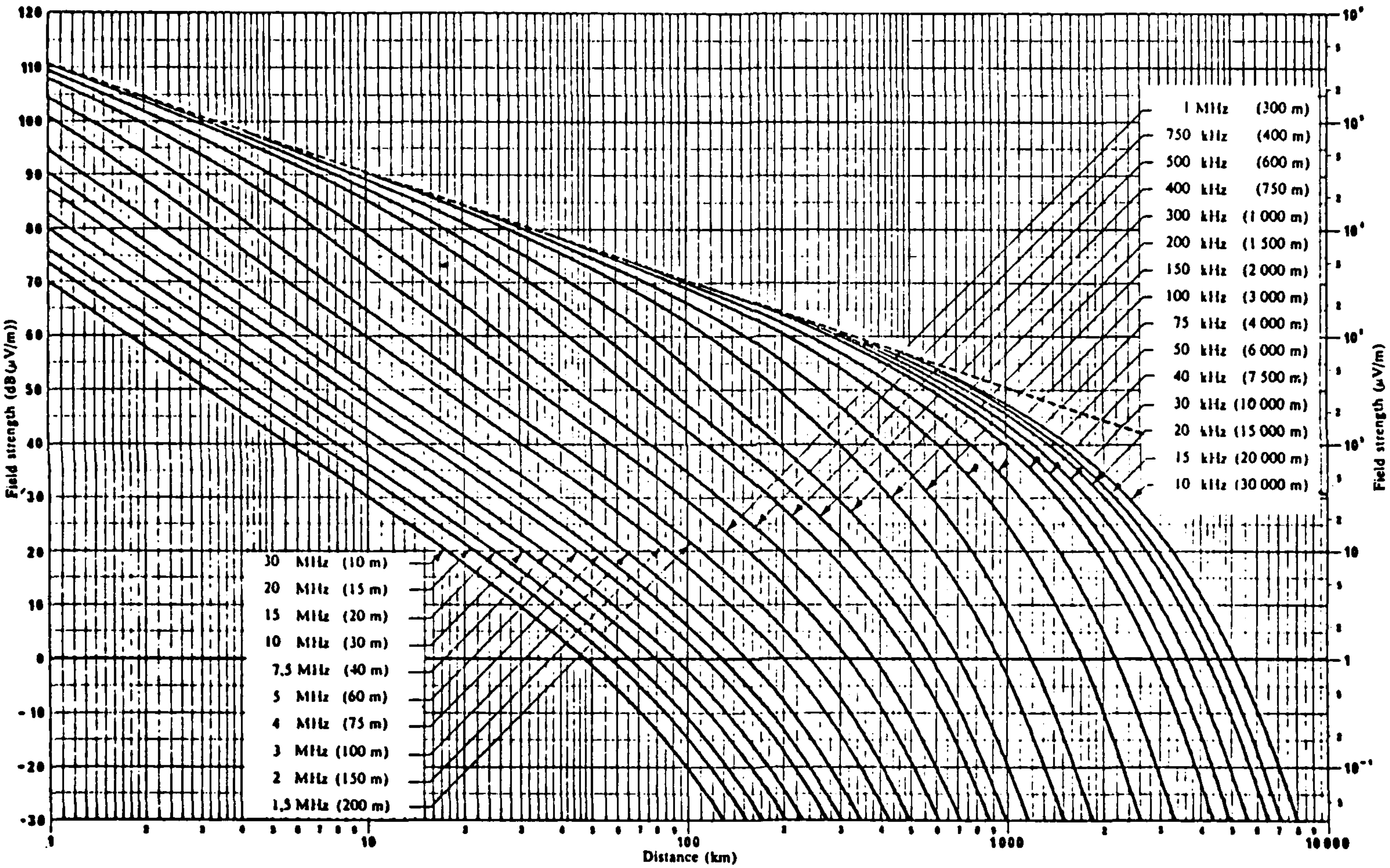

Figure A-5. Ground wave propagation curves; Land, $\sigma = 10^{-3}$ S/m, $\varepsilon = 4$.

----- Inverse distance curve

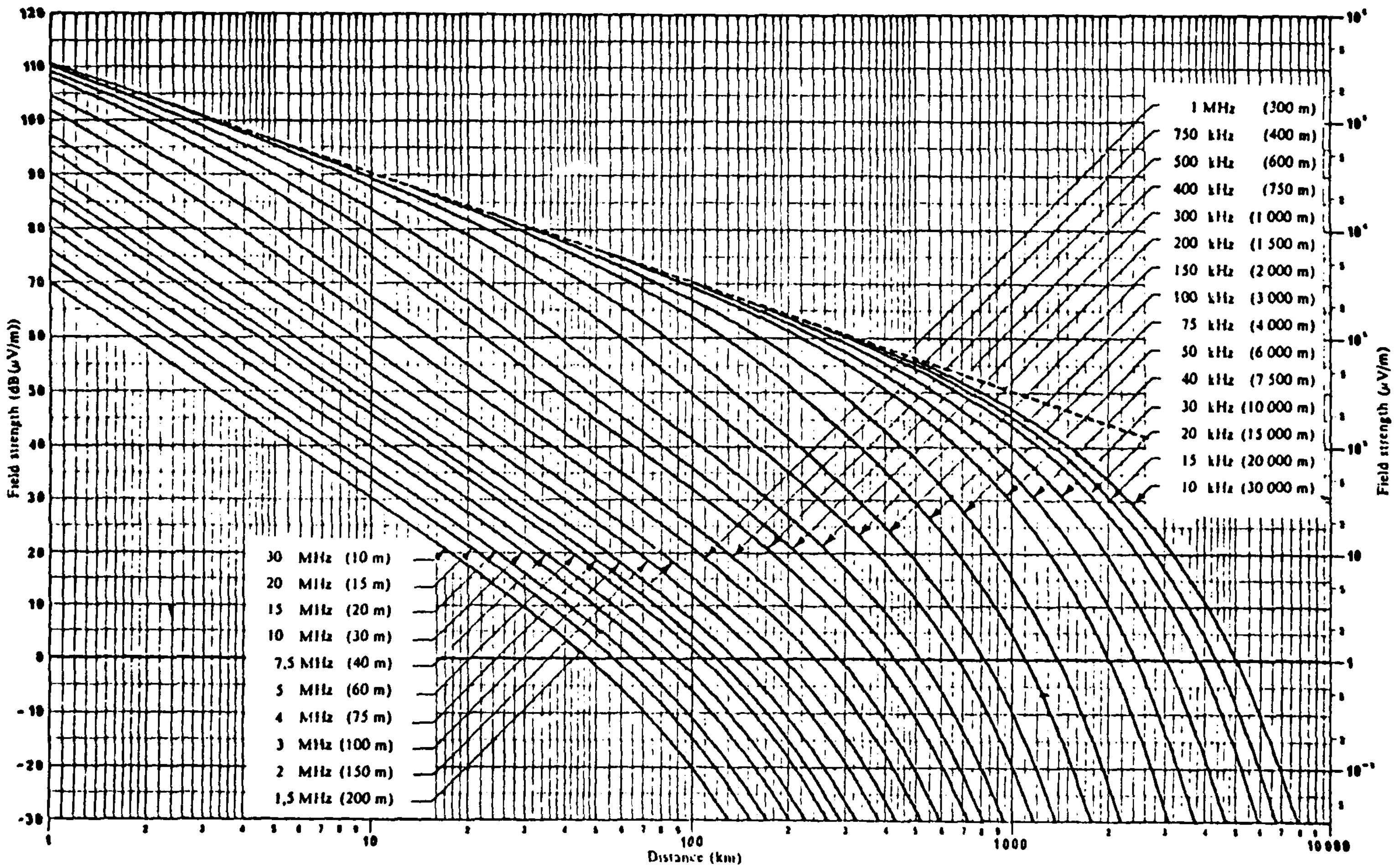

Figure A-6. Ground wave propagation curves; Land, $\sigma = 3 \times 10^{-4}$ S/m, $\varepsilon = 4$.

----- Inverse distance curve

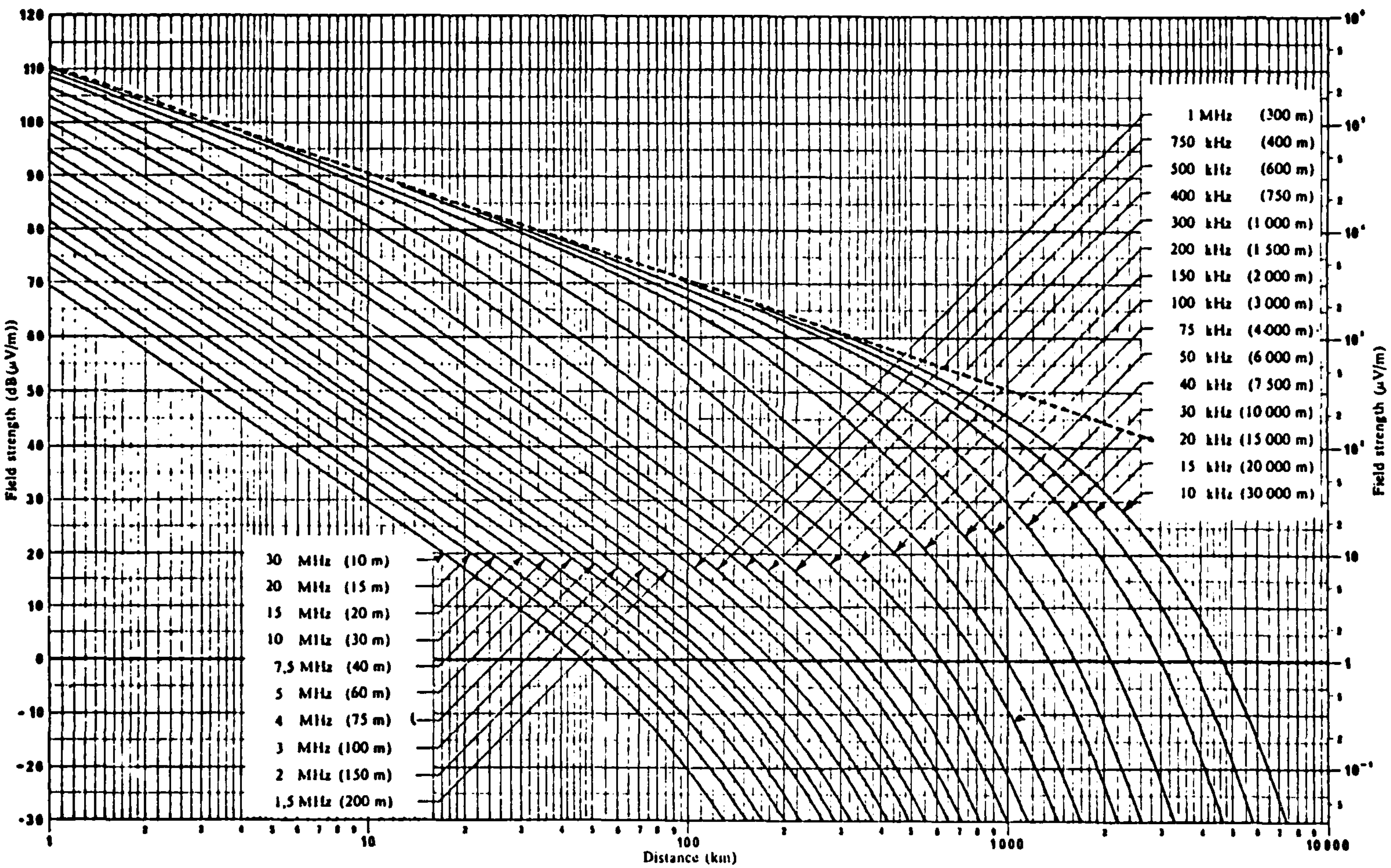

Figure A-7. Ground wave propagation curves; Land, $\sigma = 10^{-4}$ S/m, $\varepsilon = 4$.

----- Inverse distance curve

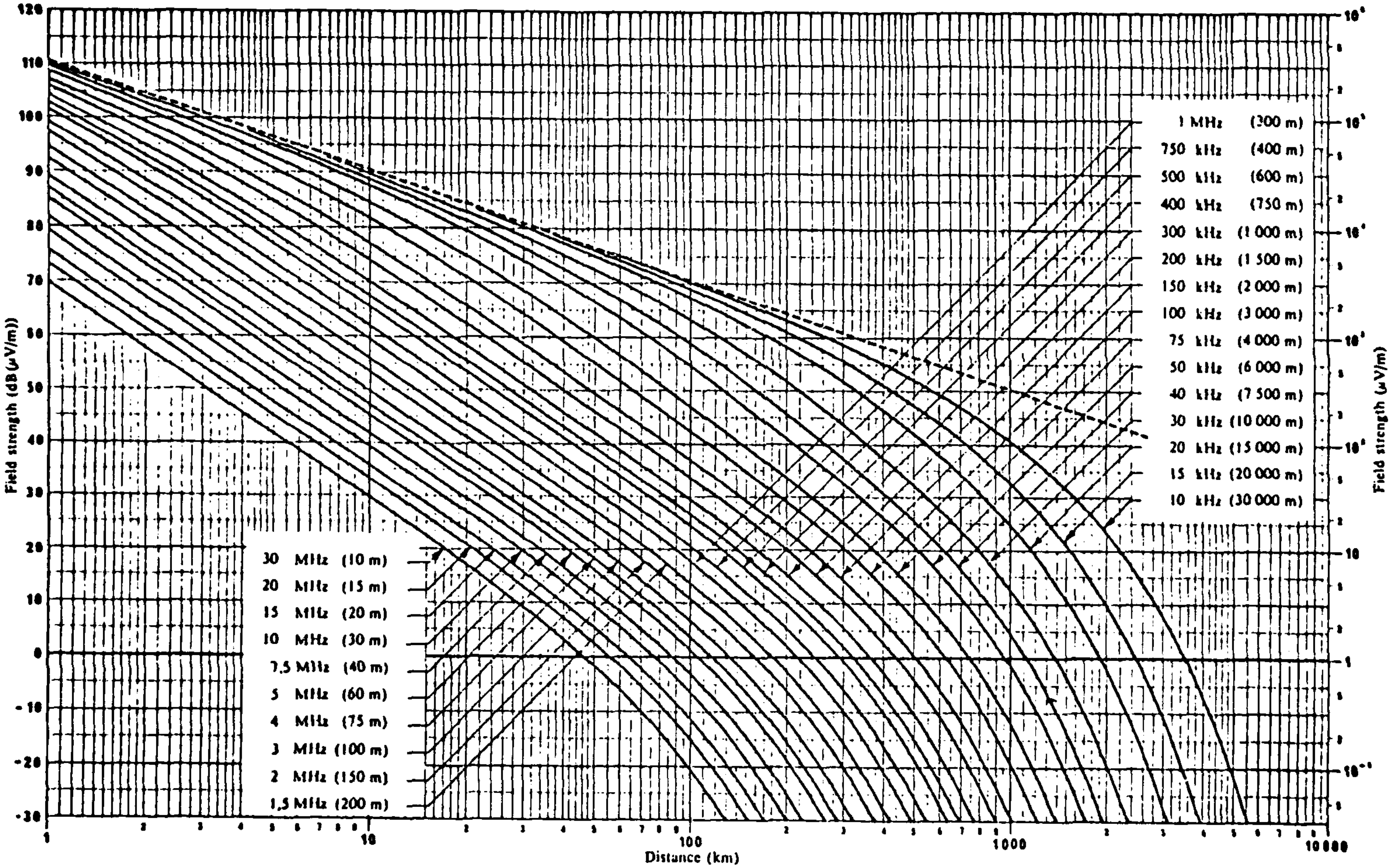

Figure A-8. Ground wave propagation curves; Land, $\sigma = 3 \times 10^{-5}$ S/m, $\varepsilon = 4$.

----- Inverse distance curve

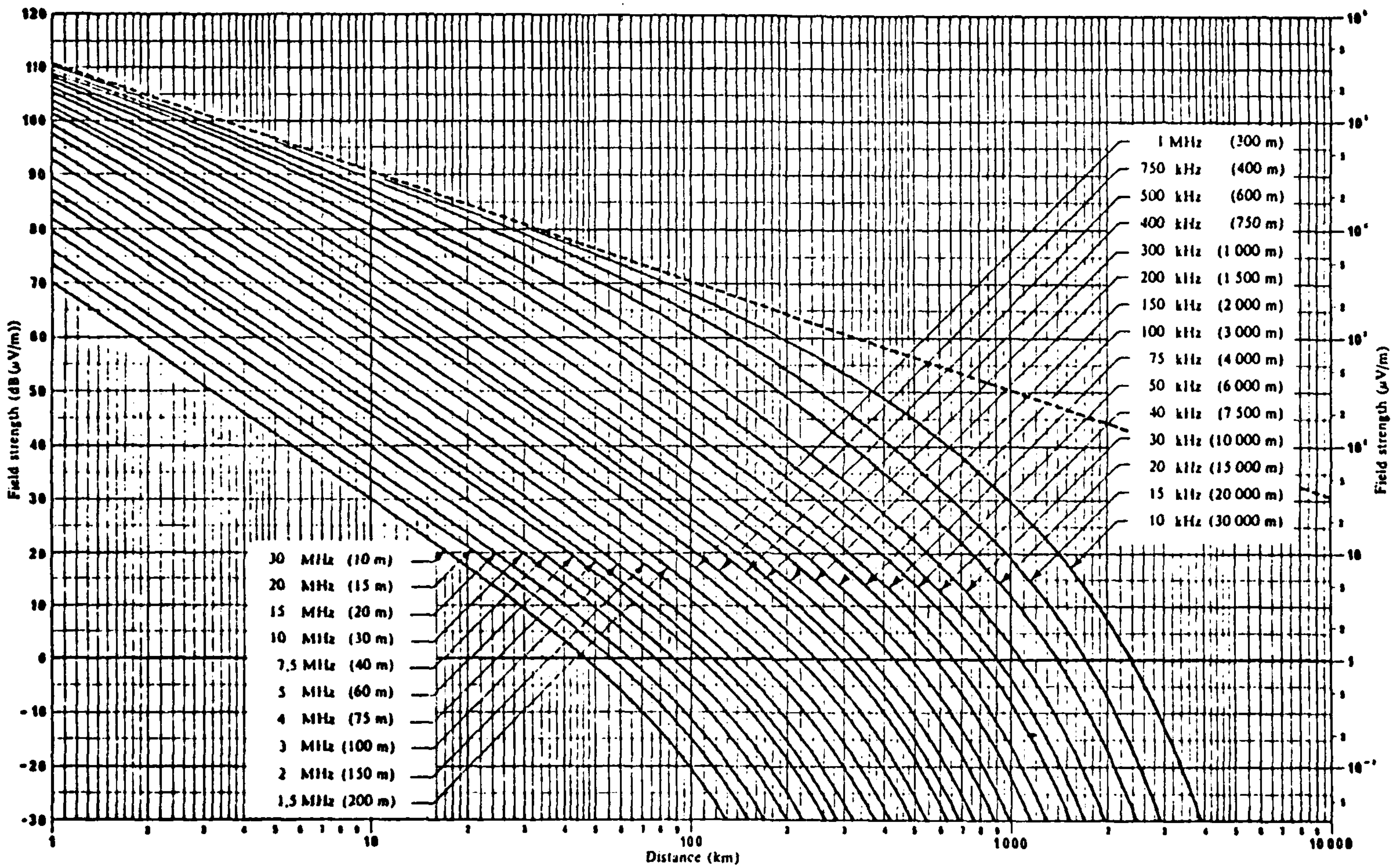

Figure A-9. Ground wave propagation curves; Land, $\sigma = 10^{-5}$ S/m, $\varepsilon = 4$.

----- Inverse distance curve

DISTRIBUTION LIST

DEPARTMENT OF DEFENSE

Command & Control Technical Center
ATTN: C-312, R. Mason
ATTN: C-650, G. Jones
3 cy ATTN: C-650, W. Heidig

Defense Communications Agency
ATTN: Code 230
ATTN: Code 205
ATTN: Code 101B

Defense Communications Engineer Center
ATTN: Code R410, N. Jones
ATTN: Code R123

Defense Intelligence Agency
ATTN: Dir
ATTN: DB-4C, E. O'Farrell
ATTN: DB, A. Wise
ATTN: DT-1B
ATTN: DC-7B

Defense Nuclear Agency
ATTN: NAFD
ATTN: NATD
ATTN: STNA
ATTN: RAEE
4 cy ATTN: TITL
6 cy ATTN: RAAE

Defense Technical Information Center
12 cy ATTN: DD

Deputy Under Secretary of Defense
Comm, Cmd, Cont & Intell
ATTN: Dir of Intelligence Sys

Field Command
Defense Nuclear Agency
ATTN: FCPR, J. McDaniel

Field Command
Defense Nuclear Agency
Livermore Branch
ATTN: FCPRL

Interservice Nuclear Weapons School
ATTN: TTV

Joint Chiefs of Staff
ATTN: C3S Evaluation Office (HD00)
ATTN: C3S

Joint Strat Tgt Planning Staff
ATTN: JLA, Threat Applications Div
ATTN: JLTW-2

National Security Agency
ATTN: R-52, J. Skillman
ATTN: B-3, F. Leonard
ATTN: W-32, O. Bartlett

Under Secretary of Defense for Rsch & Engrg
ATTN: Strat & Theater Nuc Forces, B. Stephan
ATTN: Strategic & Space Sys (OS)

DEPARTMENT OF DEFENSE (Continued)

WWMCCS System Engineering Org
ATTN: R. Crawford

DEPARTMENT OF THE ARMY

Assistant Chief of Staff for Automation & Comm
Department of the Army
ATTN: DAMO-C4, P. Kenny

Atmospheric Sciences Laboratory
U.S. Army Electronics R&D Command
ATTN: DELAS-EO, F. Niles

BMD Advanced Technology Center
Department of the Army
ATTN: ATC-T, M. Capps
ATTN: ATC-O, W. Davies

BMD Systems Command
Department of the Army
2 cy ATTN: BMDSC-HW

Deputy Chief of Staff for Ops & Plans
Department of the Army
ATTN: DAMO-RQC, C2 Div

Harry Diamond Laboratories
Department of the Army
ATTN: DELHD-NW-P
ATTN: DELHD-NW-R, R. Williams

U.S. Army Chemical School
ATTN: ATZN-CM-CS

U.S. Army Comm-Elec Engrg Instal Agency
ATTN: CCC-CED-CCO, W. Neuendorf
ATTN: CCC-EMEC-PED, G. Lane

U.S. Army Communications Command
ATTN: CC-OPS-WR, H. Wilson
ATTN: CC-OPS-W

U.S. Army Communications R&D Command
ATTN: DRDCO-COM-RY, W. Kesselman

U.S. Army Foreign Science & Tech Ctr
ATTN: DRXST-SD

U.S. Army Materiel Dev & Readiness Cmd
ATTN: DRCLDC, J. Bender

U.S. Army Nuclear & Chemical Agency
ATTN: Library

U.S. Army Satellite Comm Agency
ATTN: Document Control

U.S. Army TRADOC Sys Analysis Actvy
ATTN: ATAA-TCC, F. Payan, Jr
ATTN: ATAA-PL
ATTN: ATAA-TDC

USAMICOM
ATTN: DRSMI-YSO, J. Gamble

DEPARTMENT OF THE NAVY

COMSPTEVFOR
Department of the Navy
ATTN: Code 605, R. Berg

Joint Cruise Missiles Project Ofc
Department of the Navy
ATTN: JCMG-707

Naval Air Development Center
ATTN: Code 6091, M. Setz

Naval Air Systems Command
ATTN: PMA 271

Naval Electronic Systems Command
ATTN: PME 117-2013, G. Burnhart
ATTN: PME 106-4, S. Kearney
ATTN: Code 3101, T. Hughes
ATTN: PME 117-20
ATTN: Code 501A
ATTN: PME 106-13, T. Griffin
ATTN: PME 117-211, B. Kruger

Naval Intelligence Support Ctr
ATTN: NISC-50

Naval Ocean Systems Center
ATTN: Code 5322, M. Paulson
ATTN: Code 5323, J. Ferguson

Naval Research Laboratory
ATTN: Code 7550, J. Davis
ATTN: Code 4700
ATTN: Code 7500, B. Wald
ATTN: Code 4187
ATTN: Code 7950, J. Goodman
ATTN: Code 4780
ATTN: Code 6700, T. Coffey
ATTN: Code 6780, S. Ossakow

Naval Space Surveillance System
ATTN: J. Burton

Naval Surface Weapons Center
ATTN: Code F31

Naval Telecommunications Command
ATTN: Code 341

Office of Naval Research
ATTN: Code 414, G. Joiner
ATTN: Code 412, W. Condell

Office of the Chief of Naval Operations
ATTN: NOP 65, Strat Theater Nuc Warf Div
ATTN: OP 981N
ATTN: OP 941D

Strategic Systems Project Office
Department of the Navy
ATTN: NSP-2722, F. Wimberly
ATTN: NSP-2141
ATTN: NSP-43

DEPARTMENT OF THE AIR FORCE

Aerospace Defense Command
Department of the Air Force
ATTN: DC, T. Long

DEPARTMENT OF THE AIR FORCE (Continued)

Air Force Geophysics Laboratory
ATTN: OPR, H. Gardiner
ATTN: OPR-1
ATTN: LKB, K. Champion
ATTN: CA, A. Stair
ATTN: S. Basu
ATTN: PHP
ATTN: PHI, J. Buchau
ATTN: R. Thompson

Air Force Weapons Laboratory
Air Force Systems Command
ATTN: SUL
ATTN: NTYC
ATTN: NTN

Air Force Wright Aeronautical Lab/AAAD
ATTN: W. Hunt
ATTN: A. Johnson

Air Logistics Command
Department of the Air Force
ATTN: OO-ALC/MM

Air University Library
Department of the Air Force
ATTN: AUL-LSE

Headquarters
Air Weather Service, MAC
Department of the Air Force
ATTN: DNXP, R. Babcock

Assistant Chief of Staff
Studies & Analyses
Department of the Air Force
ATTN: AF/SASC, C. Rightmeyer
ATTN: AF/SASC, W. Keaus

Ballistic Missile Office
Air Force Systems Command
ATTN: ENSN, J. Allen

Deputy Chief of Staff
Operations Plans and Readiness
Department of the Air Force
ATTN: AFXOKCD
ATTN: AFXOXFD
ATTN: AFXOKS
ATTN: AFXOKT

Deputy Chief of Staff
Research, Development, & Acq
Department of the Air Force
ATTN: AFRDS, Space Sys & C3 Dir
ATTN: AFRDSP
ATTN: AFRDSS

Headquarters
Electronic Systems Division
Department of the Air Force
ATTN: DCKC, J. Clark

Headquarters
Electronic Systems Division
Department of the Air Force
ATTN: OCT-4, J. Deas

DEPARTMENT OF THE AIR FORCE (Continued)

Headquarters
Electronic Systems Division
Department of the Air Force
ATTN: YSM, J. Kobelski
ATTN: YSEA

Foreign Technology Division
Air Force Systems Command
ATTN: TQTD, B. Ballard
ATTN: NIIS Library

Rome Air Development Center
Air Force Systems Command
ATTN: EEP

Space Division
Department of the Air Force
ATTN: YGJB, W. Mercer

Space Division
Department of the Air Force
ATTN: YKA, D. Bolin
ATTN: YKA, S. Kennedy

Strategic Air Command
Department of the Air Force
ATTN: DCX
ATTN: XPFS
ATTN: NRT
ATTN: DCXT
ATTN: DCXR, T. Jorgensen

Rome Air Development Center
Air Force Systems Command
ATTN: OCS, V. Coyne
ATTN: TSLD

OTHER GOVERNMENT AGENCIES

Central Intelligence Agency
ATTN: OSWR/NED

Department of Commerce
National Bureau of Standards
ATTN: Sec Ofc for R. Moore

Department of Commerce
National Oceanic & Atmospheric Admin
Environmental Research Laboratories
ATTN: R. Grubb

Institute for Telecommunications Sciences
National Telecommunications & Info Admin
ATTN: W. Utlaut
ATTN: L. Berry
ATTN: A. Jean

DEPARTMENT OF ENERGY CONTRACTORS

EG&G, Inc
Los Alamos Division
ATTN: J. Colvin
ATTN: D. Wright

Lawrence Livermore National Lab
ATTN: Technical Info Dept Library
ATTN: L-389, R. Ott
ATTN: L-31, R. Hager

DEPARTMENT OF ENERGY CONTRACTORS (Continued)

Los Alamos National Laboratory
ATTN: MS 670, J. Hopkins
ATTN: MS 664, J. Zinn
ATTN: C. Westervelt
ATTN: P. Keaton
ATTN: D. Simons
ATTN: T. Kunkle, ESS-5

Sandia National Laboratories
Livermore Laboratory
ATTN: B. Murphey
ATTN: T. Cook

Sandia National Lab
ATTN: Org 4241, T. Wright
ATTN: Space Project Div
ATTN: D. Dahlgren
ATTN: Org 1250, W. Brown
ATTN: 3141
ATTN: D. Thornbrough

DEPARTMENT OF DEFENSE CONTRACTORS

Aerospace Corp
ATTN: J. Straus
ATTN: D. Olsen
ATTN: N. Stockwell
ATTN: S. Bower
ATTN: R. Slaughter
ATTN: I. Garfunkel
ATTN: V. Josephson
ATTN: T. Salmi

Analytical Systems Engineering Corp
ATTN: Radio Sciences

Analytical Systems Engineering Corp
ATTN: Security

Barry Research Corporation
ATTN: J. McLaughlin

BDM Corp
ATTN: L. Jacobs
ATTN: T. Neighbors

Berkeley Research Associates, Inc
ATTN: J. Workman

Betac
ATTN: J. Hirsch

Boeing Co
ATTN: S. Tashird
ATTN: G. Hall
ATTN: M/S 42-33, J. Kennedy

Booz-Allen & Hamilton, Inc
ATTN: B. Wilkinson

University of California at San Diego
ATTN: H. Booker

Charles Stark Draper Lab, Inc
ATTN: J. Gilmore
ATTN: D. Cox

DEPARTMENT OF DEFENSE CONTRACTORS (Continued)

Computer Sciences Corp
ATTN: F. Eisenbarth

Comsat Labs
ATTN: D. Fang
ATTN: G. Hyde

Cornell University
ATTN: M. Kelly
ATTN: D. Farley, Jr

E-Systems, Inc
ATTN: R. Berezdivin

Electrospace Systems, Inc
ATTN: H. Logston

ESL, Inc
ATTN: J. Lehman
ATTN: R. Ibaraki
ATTN: R. Heckman
ATTN: J. Marshall
ATTN: E. Tsui

General Electric Co
ATTN: G. Holliday
ATTN: A. Harcar

General Electric Co
ATTN: A. Steinmayer
ATTN: C. Zierdt

General Electric Co
ATTN: F. Reibert

General Electric Co
ATTN: G. Millman

General Research Corp
ATTN: J. Garbarino
ATTN: J. Ise, Jr

Harris Corp
ATTN: E. Knick

Horizons Technology, Inc
ATTN: R. Kruger

HSS, Inc
ATTN: D. Hansen

IBM Corp
ATTN: H. Ulander

University of Illinois
ATTN: K. Yeh

Institute for Defense Analyses
ATTN: H. Gates
ATTN: J. Aein
ATTN: E. Bauer
ATTN: H. Wolfhard

International Tel & Telegraph Corp
ATTN: W. Rice
ATTN: Technical Library

DEPARTMENT OF DEFENSE CONTRACTORS (Continued)

JAYCOR
ATTN: J. Sperling

JAYCOR
ATTN: J. Doncarlos

Johns Hopkins University
ATTN: T. Potemra
ATTN: J. Phillips
ATTN: T. Evans
ATTN: J. Newland
ATTN: P. Komiske

Kaman Sciences Corp
ATTN: T. Stephens

Kaman Tempo
ATTN: DASIAC
ATTN: W. Knapp
ATTN: W. McNamara

Linkabit Corp
ATTN: I. Jacobs
ATTN: A. Viterbi
ATTN: H. Van Trees

Litton Systems, Inc
ATTN: R. Grasty

Lockheed Missiles & Space Co, Inc
ATTN: W. Imhof
ATTN: R. Johnson
ATTN: M. Walt

Lockheed Missiles & Space Co, Inc
ATTN: C. Old, Dept 68-21
ATTN: D. Churchill, Dept 81-11
ATTN: Dept 60-12

M.I.T. Lincoln Lab
ATTN: D. Towle

Magnavox Govt & Indus Electronics Co
ATTN: G. White

Martin Marietta Corp
ATTN: R. Heffner

McDonnell Douglas Corp
ATTN: H. Spitzer
ATTN: W. Olson
ATTN: R. Halprin

Meteor Communicatons Consultants
ATTN: R. Leader

Mission Research Corp
ATTN: R. Kilb
ATTN: Tech Library
ATTN: D. Sappenfield
ATTN: F. Fajen
ATTN: R. Hendrick
ATTN: R. Bogusch
ATTN: S. Gutsche
4 cy ATTN: G. Fulks
5 cy ATTN: Doc Con

DEPARTMENT OF DEFENSE CONTRACTORS (Continued)

Mitre Corp
ATTN: B. Adams
ATTN: G. Harding
ATTN: A. Kymmel
ATTN: C. Callahan

Mitre Corp
ATTN: M. Horrocks
ATTN: W. Foster
ATTN: W. Hall
ATTN: J. Wheeler

Pacific-Sierra Research Corp
ATTN: F. Thomas
ATTN: E. Field, Jr
ATTN: H. Brode, Chairman SAGE

Pennsylvania State University
ATTN: Ionospheric Research Lab

Photometrics, Inc
ATTN: I. Kofsky

Physical Dynamics, Inc
ATTN: E. Fremcuw

Physical Research, Inc
ATTN: R. Deliberis

R & D Associates
ATTN: F. Gilmore
ATTN: B. Gabbard
ATTN: M. Gantsweg
ATTN: W. Karzas
ATTN: W. Wright
ATTN: C. Greifinger
ATTN: R. Lelevier
ATTN: H. Ory
ATTN: R. Turco
ATTN: P. Haas

R & D Associates
ATTN: B. Yoon

Rand Corp
ATTN: E. Bedrozian
ATTN: C. Crain

Riverside Research Institute
ATTN: V. Trapani

Rockwell International Corp
ATTN: R. Buckner

Rockwell International Corp
ATTN: S. Quilici

DEPARTMENT OF DEFENSE CONTRACTORS (Continued)

Santa Fe Corp
ATTN: D. Paolucci

Science Applications, Inc
ATTN: C. Smith
ATTN: L. Linson
ATTN: D. Hamlin
ATTN: E. Straker

Science Applications, Inc
ATTN: SZ

Science Applications, Inc
ATTN: J. Cockayne

SRI International
ATTN: A. Burns
ATTN: R. Livingston
ATTN: R. Leadabrand
ATTN: D. Neilson
ATTN: M. Baron
ATTN: W. Chesnut
ATTN: R. Tsunoda
ATTN: G. Smith
ATTN: G. Price
ATTN: C. Rino
ATTN: W. Jaye
ATTN: J. Petrickes

Sylvania Systems Group
ATTN: J. Concordia
ATTN: I. Kohlberg
ATTN: R. Steinhoff

Technology International Corp
ATTN: Doc Con for W. Boquist

Tri-Com, Inc
ATTN: D. Murray

TRW Electronics & Defense Sector
ATTN: R. Pleubuch
ATTN: D. Dee

Utah State University
ATTN: K. Baker
ATTN: L. Jensen
ATTN: J. Dupnik

Visidyne, Inc
ATTN: C. Humphrey
ATTN: J. Carpenter